# Myofibroblasts Induce Ectopic Activity in Cardiac Tissue

*Michele Miragoli, Nicolò Salvarani and Stephan Rohr*

*(Circ. Res. 2007;101:755-758)*

## State of the art

### Fibroblasts: physiological phenotype

Whereas cardiomyocytes are the dominant cell type in the normal heart in respect to volume, more than half of the cells consist of noncardiomyocytes, among which fibroblasts constitute a significant fraction (Adamson et al., 2005). In normal human hearts, fibroblasts outnumber cardiomyocytes by a factor of ~ 2-3 while occupying ~20 % of the volume of the working myocardium. Under physiological conditions, fibroblasts are responsible for providing cardiomyocytes with a mechanical scaffold, which integrates the contractile activity of individual cells so as to result in the coordinated pump function of the organ. Accordingly, fibroblasts are found throughout the myocardium, where they form a 3D cellular network surrounding groups of cardiomyocyte (Goldsmith et al., 2004). Fibroblasts produce a network of collagen fibers and integrates the mechanical forces as to result in an efficient pump function of the entire organ. This fibrillar network is subjected to substantial turnover which can amount up to ~ 5% per day (McAnulty et al., 1987). Under physiological conditions, tight control of formation and degradation of collagen is therefore necessary to maintain the structural and functional integrity of the myocardium over time. The integrity of this structure is adversely affected by a large number of cardiac diseases ranging from volume to pressure overload and to myocardial infarction. Under pathological conditions the delicate balance between formation and degradation of collagen tips towards an accumulation of extracellular matrix (ECM) which is caused by increased secretory activity and proliferation of fibroblasts.

Morphologically, this situation is characterized by an initial reactive perivascular fibrosis which subsequently extends into the interstitium. It has been shown that reactive fibrosis is related to inappropriate and chronic elevations of circulating hormones such as angiotensin II, aldosterone and endothelin-1 which act in tandem with fibrogenic cytokines like transforming growth factor b1 (TGF-β1) and connective tissue growth factor (CTGF) (Weber et al., 2000). Under these pathological conditions, complex reactions involving changes in extracellular matrix production, cell proliferation, and cell death cause structural remodeling of the ventricular wall, which compromises pump function and predisposes the heart to arrhythmias (Peters et al., 1998). It is well established that fibroblasts, by producing collagenous septa in the aged and hypertrophied heart, generate electrical barriers, which form the basis of discontinuous conduction and, hence, a substrate for arrhythmias (Swynghedauw et al., 1999). However, it is not known whether fibroblasts populating the collagenous septa might directly affect the electrophysiological properties of adjacent myocardium by forming electrical contacts with cardiomyocytes. Electrical coupling between cardiomyocytes and fibroblasts was demonstrated many decades ago in cell cultures and, more recently, in intact tissue. In cell cultures, it has been shown that single fibroblasts are capable of synchronizing contraction among individual cardiomyocytes and that these contractions are accompanied by synchronous membrane potential fluctuations in the interconnecting fibroblasts, suggesting the presence of electrical communication (Hyde et al., 1969). More recently, it has been shown in a cell culture model consisting of fibroblasts grafted on top of monolayer cultures of cardiomyocytes that the former were able to modify the local electrophysiological properties of cardiomyocytes, suggesting the presence of electrical coupling between the two cell types (Feld et al., 2002). In intact tissue, evidence has been presented that mechanosensitive fibroblasts in the sinoatrial region are electrically coupled to atrial cardiomyocytes (Kohl et al., 1994). All of these studies concerned electrical short-range interactions between cardiomyocytes and adjacent individual fibroblasts. The possibility that multiple fibroblasts might interact electrically over extended distances with cardiomyocytes was shown in the department of physiology of Bern by the published paper “Coupling of cardiac activity over extended distances by fibroblasts of cardiac origin” (Gaudesius et al., 2003). Long-range interactions between fibroblasts and cardiomyocytes were investigated using a novel cell culture

system that permitted the generation of geometrically defined heterocellular preparations consisting of cardiomyocytes and noncardiomyocytes (Figure 1).
In this work is demonstrated that fibroblasts of cardiac origin are able to synchronize electrical activity between remote areas of cardiac origin tissue for distances up to 300 µm. With increasing distance, synchronization along fibroblasts was increasingly delayed by up to ~ 70 ms, thus resulting in extremely slow local 'conduction velocities' and, accordingly, in highly discontinuous conduction (Figure 2 and Figure 3). Electrical synchronization was also supported by Cx43 transfected HeLa cells (but not by communication deficient HeLa wild-type cells) indicating that not the cell type *per se* but its ability to establish heterocellular gap junctional coupling was essential for non-excitable cells to support impulse transmission. Immunocyto-chemical determination of connexin expression showed that gap junctional coupling of fibroblasts to cardiomyocytes was based on Cx43 and Cx45 (Figure 4). These findings support the concept that fibroblasts in intact hearts might influence the spatial patterns of electrical activation not only by producing electrical barriers consisting of collagenous septa, but also by direct modulation of active and passive electrical properties of the network of cardiomyocytes which ultimately results in slow and discontinuous conduction. Such long-range interactions may explain synchronization of electrical activity across scar tissue between donor and recipient cardiac tissue after heart transplantation and may be a cause of ensuing arrhythmias (Lefroy et al., 1998). More important, in the setting of cardiac fibrosis, bridges consisting of fibroblasts might establish focal electrical connections across collagenous septa, which may contribute to the generation of arrhythmias by forming slow pathways of excitation.

## Myofibroblasts: physiopathological phenotype

Both reactive fibrosis as well as reparative fibrosis occurring in the context of infarction are typically accompanied by the appearance of so-called myofibroblasts which is considered to be an essential step in the establishment of fibrosis (Weber et al., 2004). Myofibroblasts were first described as fibroblastic cells located within granulation tissue of skin wounds where they initiate contraction of the granulation tissue and disappear thereafter by programmed cell death (Gabbiani et al., 2003). Myofibroblasts express several smooth muscle cell markers among which a-smooth

muscle actin (α-SMA) is considered to be the most reliable immunocytochemical marker (Tomasek et al., 2002). In the heart, myofibroblasts are not normally present. This situation, however, changes drastically under pathological conditions. In animal models of pressure overload, it was shown that early inflammatory changes are followed by myofibroblast proliferation within days and the subsequent development of perivascular and interstitial fibrosis (Tokuda et al., 2004). Similarly, at sites of myocardial infarctions, myofibroblasts appear a few days after the ischemic event in very large numbers and, due to incomplete apoptosis during the healing process, locally persist for many years. Myofibroblasts in infarcts are of central importance for both the initial scar formation and the continuous rebuilding of the scar thereafter (Sun et al., 2006). Based on previous studies showing that myofibroblasts express connexins in tissues other than heart (Gabbiani et al., 1978), the question arises whether this cell type might similarly be capable of forming functional gap junctions in diseased myocardia. If this were to be the case, the intriguing possibility arises that myofibroblasts might be involved in arrhythmogenesis not only by contributing to the formation of electrically insulating collagenous septa causing discontinuous and zig-zag conduction (Spach et al., 1997) but also by direct electrotonic modulation of impulse conduction. While the exact origin of myofibroblasts is still not entirely clear there is ample evidence that their appearance is triggered by a local inflammatory reaction, mechanical stress and humoral factors. In regard to humoral factors, induction of myofibroblasts is triggered in particular by TGF-β1, but other factors such as basic fibroblast growth factor (bFGF/FGF-2), angiotensin II (AngII), catecholamines, and insulin-like growth factor-1 (IGF-1) are involved in the determination of phenotype and function of cardiac fibroblasts as well (Manabe et al., 2002). Apart from being the target for humoral factors, myofibroblasts themselves produce a wide variety of growth factors and cytokines (e.g., bFGF, PDGF, TGF-β, endothelin-1, interleukin-1, tumor necrosis factor α) which act in both autocrine and paracrine fashion and possibly establish a way to communicate with cardiomyocytes. The circumstance that myofibroblasts, in concert with altered levels of humoral factors, most likely play a central role in structural cardiac remodeling is exemplified by the observation that AngII (which is also produced locally by the expression of functional ACE by the myofibroblasts) induces $AT_1$-receptor mediated increase of collagen synthesis leading to reactive cardiac fibrosis

(Weber et el., 2000).

## Arrhythmias and the role of (myo)fibroblasts

It emerges that there exists a vast consensus regarding the pivotal role of myofibroblasts in structural remodeling of the extracellular matrix in injured hearts. But what about their role in arrhythmias? In principle, there exist three possibilities whereby myofibroblasts might be involved in arrhythmogenesis: (1) by contributing to the excessive deposition of extracellular matrix, myofibroblasts cause arrhythmogenic slow and discontinuous impulse conduction and conduction blocks; (2) given the paracrine secretion of a myriad of growth factors and cytokines (Powel et al., 1999), myofibroblasts might cause arrhythmogenic remodeling of the cellular electrophysiology of neighboring cardiomyocytes. These interactions might occur in intact tissue is suggested by the effects of some myofibroblast-produced humoral factors on cellular cardiac electrophysiology: for example, (2.1) tumor necrosis factor-α (TNF-α) inhibits the delayed rectifier and the transient potassium outward current ($I_{to}$) (Kawada et al., 2006); (2.2) insulin-like growth factor (IGF-1) upregulates expression of L-type calcium channels (Sun et al., 2006); (2.3) transforming growth factor b1 (TGF-β1) finally was shown to downregulate $I_{Ca\text{-}L}$ in atrial cardiomyocytes (Avila et al., 2007); (3) by establishing gap junctional communication with cardiomyocytes, myofibroblasts might adversely influence the cellular electrophysiology of cardiomyocytes by direct electrotonic interactions. This last possibility is obviously dependent on the capability of myofibroblasts to establish heterocellular gap junctional coupling in the working myocardium. In the intact heart, investigations into the possibility of gap junctional coupling between fibroblasts and cardiomyocytes in healthy myocardia produced controversial results. While one study showed homo-and heterocellular connexin expression by fibroblasts in neonatal rat ventricles (Cx43 and Cx45) (Goldsmith et al., 2004), another investigation performed with sheep ventricular tissue found no immunocytochemical evidence for fibroblasts related Cx43 expression. Interestingly, however, the latter study reported that fibroblasts residing in infarct scars show abundant expression of Cx43 and Cx45 (Camelliti et al., 2004). By combining this finding with the results of other immunohistochemical studies showing that fibroblasts in infarct scars are in

fact myofibroblasts, it is quite likely that the connexin expressing 'fibroblasts' observed in infarct scars in the former study were in fact connexin expressing myofibroblasts (Sun et al., 1996). This raises the very interesting perspective that myofibroblasts occurring in diseased hearts might be capable of establishing gap junctional coupling both among themselves and with cardiomyocytes thereby contributing to arrhythmogenesis much more directly than previously thought. In the department of physiology of Bern was investigated whether impulse propagation along strands of cultured cardiomyocytes might be affected by the presence of cardiac fibroblasts by the published papaer “Electrotonic modulation of cardiac conduction by myofibroblasts” (Miragoli et al., 2006). The possibility that fibroblasts modulate the electrical properties of multicellular cardiac tissue was subsequently investigated by coating strands of cultured cardiomyocytes with a layer of fibroblasts (Figure 5). Because it is not feasible to directly assess myofibroblasts - cardiomyocyte interactions in intact tissue due to limitations of presently available methodologies, it was used patterned growth primary cell cultures instead where the spatial interaction between both cell types can be closely controlled and where either cell type can be clearly identified. Whereas it has been reported before that cardiac fibroblasts in culture undergo a phenotype switch to myofibroblasts due to the mechanical stress exerted by the rigid cultures substrates, it was shown in the study that, also when cultured on top of 'soft' cardiomyocytes, fibroblasts undergo a transition to α-smooth muscle actin (α-SMA) positive myofibroblasts which express Cx43 and Cx45 at both homo- and hetero-cellular cell contacts (Figure 6). Moreover, it was found that with increasing myofibroblast density, maximal upstroke velocities and conduction velocities along the cardiomyocyte strands first slightly increased and then decreased reaching ~ 50% of control values upon complete coverage with myofibroblasts. This biphasic behavior was highly reminiscent of the phenomenon of supernormal conduction as observed during gradual depolarization of cardiac tissue with potassium (Shaw et al., 1997) and suggested that myofibroblasts induced a density dependent gradual depolarization of cardiomyocytes towards levels of membrane potentials giving rise to slow $I_{Ca\text{-}L}$ based conduction (Figure 7 and Figure 8). Measurements of membrane potentials using sharp intracellular impalements showed that this was indeed the case with maximal diastolic potentials decreasing from ~ -80 mV to ~ -50 mV upon full coverage of the cardiomyocyte strands with myofibroblasts (Figure 9). These results open the perspective that heterocellular

electrotonic interactions between cardiomyocytes and myofibroblasts might be involved in the generation of arrhythmogenic ectopic activity which, together with myofibroblasts induced slow and discontinuous conduction, might turn remodeled cardiac tissue into a highly arrhythmogenic substrate.

## Ectopic Activity

Focal ectopic activity in cardiac tissue is a key factor in the initiation and perpetuation of tachyarrhythmias (Gorenek et al., 2003). In fact, the majority of ventricular tachycardias in non-ischemic heart failure and a fraction of tachycardias in ischemic heart failure are thought to be based on ectopic pacemakers firing at a rate faster than the sinus node (Rubart et al., 2005). Moreover, premature ectopic beats can trigger the establishment of reentrant electrical activity underlying atrial and ventricular tachyarrhythmias. The origin and the mechanisms of ectopic activity vary in different parts of the heart. In the case of atrial fibrillation (AF), it has been shown that ectopic activity arising at the muscular sleeves that extend into the atrial veins play an important role (Tsai et al., 2000). Accordingly, ablation of these sleeves has become a widely accepted procedure to prevent recurrence of AF even though the exact nature of the cell types and the cellular electrophysiological mechanisms underlying ectopic activity are still a matter of debate (Coutu et al., 2006). In the ventricles, ectopic activations have been shown to originate in the endocardium or epicardium in non-ischemic heart failure and at the borderzone of acute infarcts. Whereas ectopic activity in non-ischemic heart failure is based on early and/or delayed afterdepolarizations (EADs, DADs) secondary to intracellular calcium handling dysfunction (Yano et al., 2005), ectopic activity arising at the borderzone of acute infarcts is thought to involve, besides injury currents, activation of mechano-sensitive ion channels (Coronel et al., 2002). Ectopic activity has recently also become an issue in the context of cardiac cell therapy which holds substantial promise for improving heart function in a variety of disease settings. It was shown in several studies both *in-vitro* and *in-vivo* that cell transplants might unfortunately also bear arrhythmogenic risks (Abraham et al., 2005). Whereas spontaneously active cell grafts are in fact desired in the context of constructing biological pacemakers (Xue et al., 2005), spontaneous activity of grafted cells is

clearly unwanted if not fatal in the context of cell transplantation with the goal of improving mechanical function of the heart. In principle, spontaneous ectopic activity following cell transplantation can be a feature of the transplanted cells themselves or can be based on heterocellular interactions with surrounding cardiomyocytes based on either direct electrotonic coupling and/or paracrine action between the transplanted cells and cardiomyocytes. Examples of such modulations of excitability investigated *in-vitro* include the demonstration that growing single cardiomyocytes on communication deficient fibroblasts increases excitability and that coating of cardiomyocytes with Kv1.3 transfected and communication competent fibroblasts induces discontinuous conduction and conduction blocks (Kizana et al., 2006). Apart from intact hearts, 'ectopic' activity also occurs in cardiomyocytes *in-vitro*. In fact, the hallmark of monolayer cultures of ventricular cardiomyocytes, i.e., their spontaneous beating, is an example of ectopic activity given that the ventricular cardiomyocytes do not normally show autorhythmicity under physiological conditions. Spontaneous contractile activity in cardiac cell cultures was first described nearly 100 years ago by Burrows in 1912. Even though never investigated in detail ever since, automaticity in cultured cardiomyocytes is generally assumed to be due to a dedifferentiation of ventricular cardiomyocytes towards a fetal phenotype which is accompanied by the expression of ion channels and exchangers permitting occurrence of pacemaking. In contrast and as outlined in more detail below, we recently made the surprising observation that spontaneous ectopic activity in primary cultures of cardiomyocytes is in fact not primarily due to a dedifferentiation of cardiomyocytes, but that it is critically dependent on the presence of 'contaminating' myofibroblasts which are coupled by gap junctions to cardiomyocytes. Because, as outlined in the introduction, myofibroblasts are nearly omnipresent in structurally remodeled diseased myocardia, our observation of myofibroblast induced ectopic activity then raises the important question whether, also in intact hearts, myofibroblasts might modulate cardiomyocyte excitability to an extent which would favor appearance of ectopic activity.

# Mechanisms by which Myofibroblasts could evoke Ectopic Activity

A part from the possibility that paracrine effects may involved, differences in intrinsic membrane potentials of myofibroblast vs. cardiomyocytes are likely to play an important role as mechanisms by which myofibroblasts could evoke ectopic activity. These differences were measured for the first time nearly 4 decades ago by Girardier et al. who reported, using intracellular recordings with sharp electrodes, that the resting potential of cultured cardiomyocytes and fibroblasts were ~ -63 mV and ~ -35 mV, respectively, and that, if cultured together at equal densities, the potential of both cell types took on an intermediate value amounting to ~ -50 mV (Hyde et al., 1969). These observations were later confirmed using patch clamp techniques (Rook et al., 1989). Based on these findings, it can be hypothesized that, at rest, there is a depolarizing current flow from myofibroblasts to coupled cardiomyocytes which could evoke ectopic activity based on the same mechanism as that underlying ectopic activity produced by injury currents flowing across the border of acutely ischemic tissue (Coronel et al., 1991). There, abnormal impulse generation is based on current flowing from the depolarized ischemic tissue to adjacent normal cardiac tissue which, as a consequence, undergoes graded depolarization. Depending on the magnitude of this depolarizing injury current, the excitability of the normal tissue adjacent to the ischemic region is either increased (subthreshold) or, if suprathreshold, an ectopic beat is elicited. This situation was recently reproduced in a study using a depolarized cell model coupled to a real Purkinje cell where setting the potential of the model cell such that Purkinje cells were depolarized to ~ -55 mV resulted in spontaneous activity which was abolished by L-type calcium current ($I_{Ca-L}$) blockers (Huelsing et al., 2003). This value is close to values reported previously for cardiomyocyte-fibroblast pairs and suggests that partial depolarization of cardiomyocytes by myofibroblasts is likely to be involved in the generation of spontaneous activity.

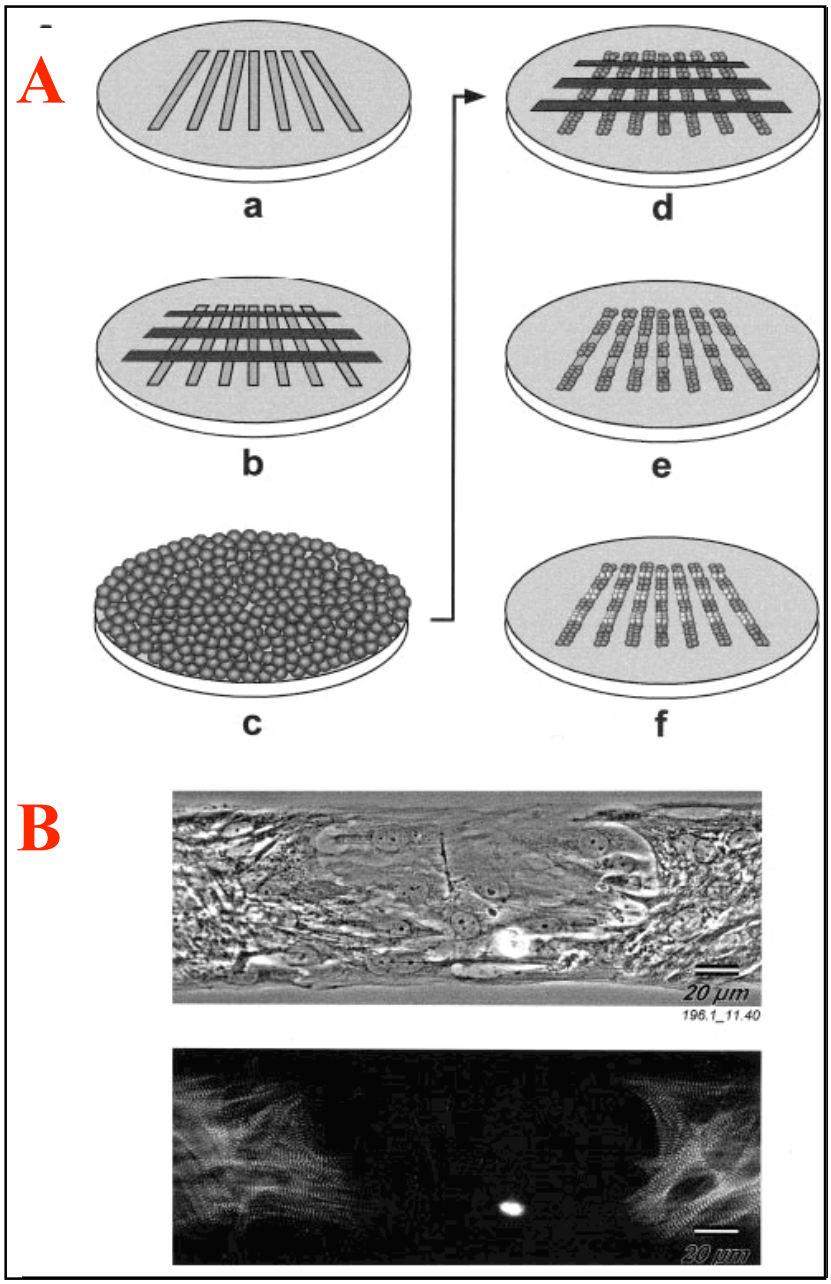


***Figure 1. Preparation of geometrically defined heterocellular cultures.*** *A, Strips of collagen on agar-coated glass coverslips were prepared using previously published photolithographic techniques (Rohr et al., 1998 and 2003) (a). The collagen strips were masked at defined locations with adhesive tapes (b), and freshly dissociated cardiomyocytes were seeded and left to attach for 24 hours (c). Washing away unattached cells resulted in strands of cardiomyocytes interrupted over defined distances by the tapes (d). Removal of the tapes reexposed the collagen (e) and permitted cells different from cardiomyocytes to fill the gaps in the strands after a second seeding step (f). B, Example of an approximately 80-µm-long fibroblast insert is shown. As illustrated by the phase-contrast image, fibroblasts (translucent cytoplasm) completely filled the gap in the myocyte strand. The corresponding immunofluorescent image obtained after staining with anti-myomesin shows absence of cardiomyocytes in the gap and permitted the exact assessment of the insert length.*

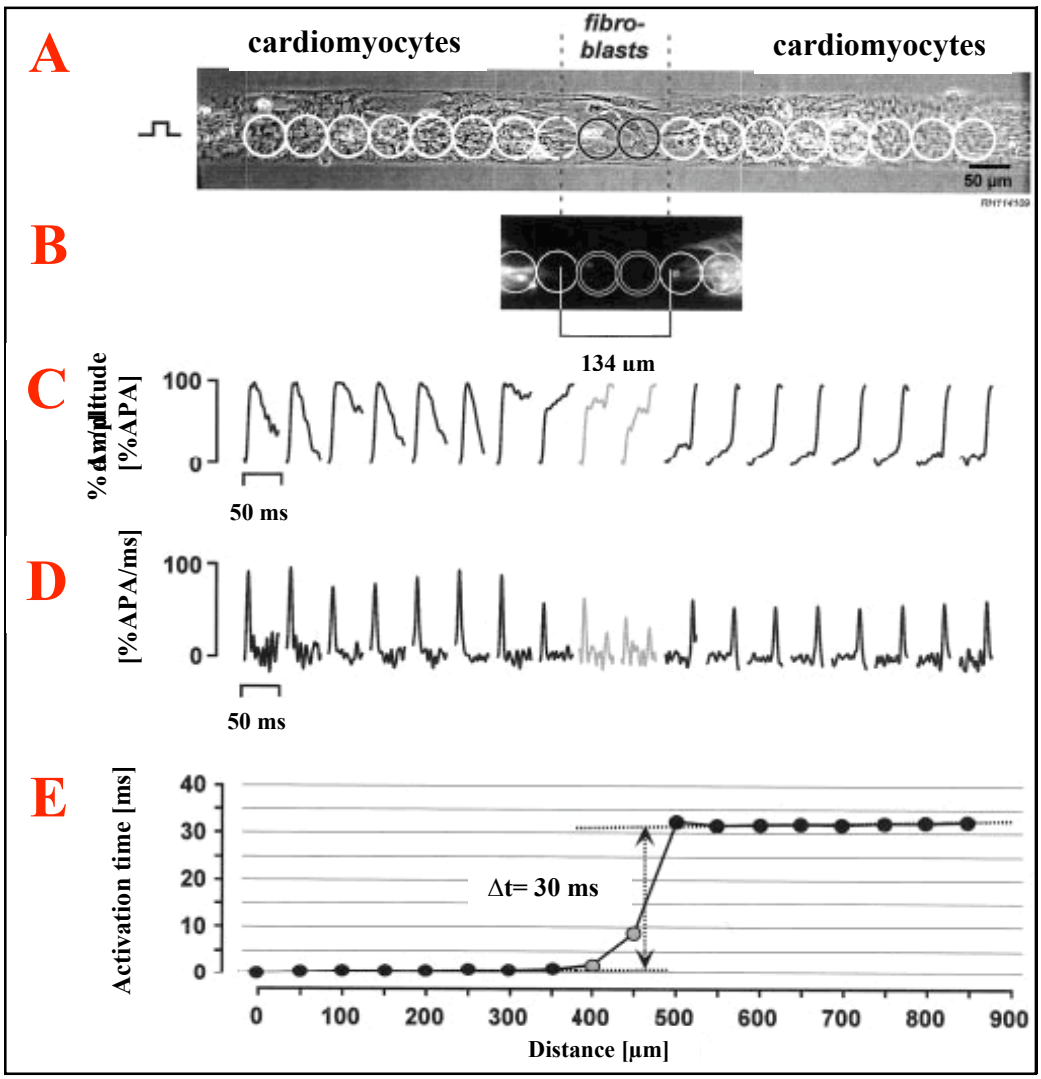


***Figure 2. Characteristics of impulse propagation across a fibroblast insert.*** *A, Phase-contrast image of the preparation consisting of an 80-µm-wide strand of cardiomyocytes with a central fibroblast insert. Circles indicate the position of individual photodetectors. B, Anti-myomesin staining shows that the detectors flanking the central two detectors (black and white circles) received a mixed input from both cardiomyocytes and fibroblasts and that the overall insert length was 134 µm. C, Propagating action potentials recorded along the preparation after stimulation on the left show biphasic upstrokes in the region of the fibroblasts that are typical of bidirectional electrotonic interaction with the proximal and distal cardiomyocyte strands. D, Upstroke velocities exhibit double peaks in the region of the fibroblasts, and $dV/dt_{max}$ is diminished in the distal compared with the proximal cardiomyocyte strand. E, Plot of activation times along the preparation indicates the presence of a delay in the region of the fibroblasts.*

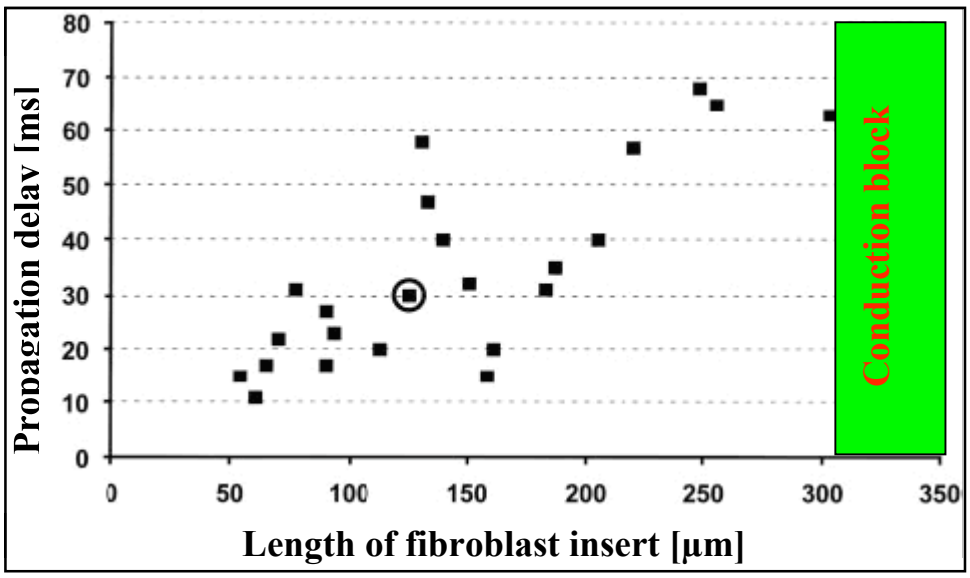


***Figure 3. Activation delays as a function of insert length.*** *Delays across fibroblast inserts were positively correlated with the length of the inserts. At insert lengths >302 µm, impulse propagation failed. The data point with a circle corresponds to the experiment shown in Figure 2.*

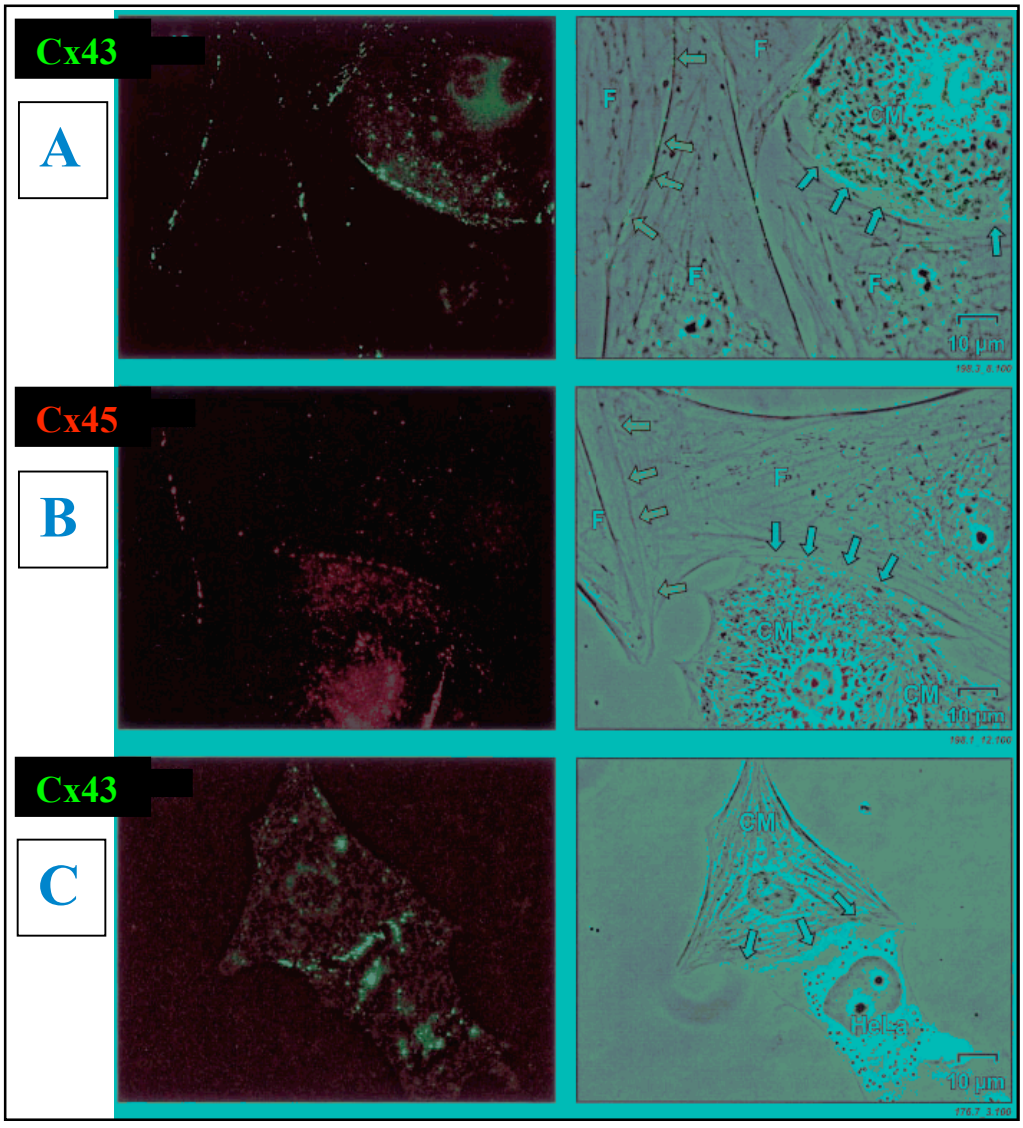


***Figure 4. Types of connexins expressed at heterocellular junctions.*** *CM indicates cardiomyocyte; F, fibroblast. A, Cx43 expression in mixed cardiomyocyte-fibroblast cultures. As shown by both the immunofluorescence image (left) and the overlay of this image with the phasecontrast picture (right), there is a distinct labelling for Cx43 in the region of abutment of the two cell types (blue arrows) and also at homocellular fibroblast junctions (yellow arrows). B, Cx45 is expressed both at homocellular fibroblast junctions (yellow arrows) and fibroblastcardiomyocyte junctions (blue arrows). C, Cx43 expression in cardiomyocyte-HeLaCx43 cell pair shows a distinct labeling for Cx43 in the region of abutment of the two cell types (blue arrows).*

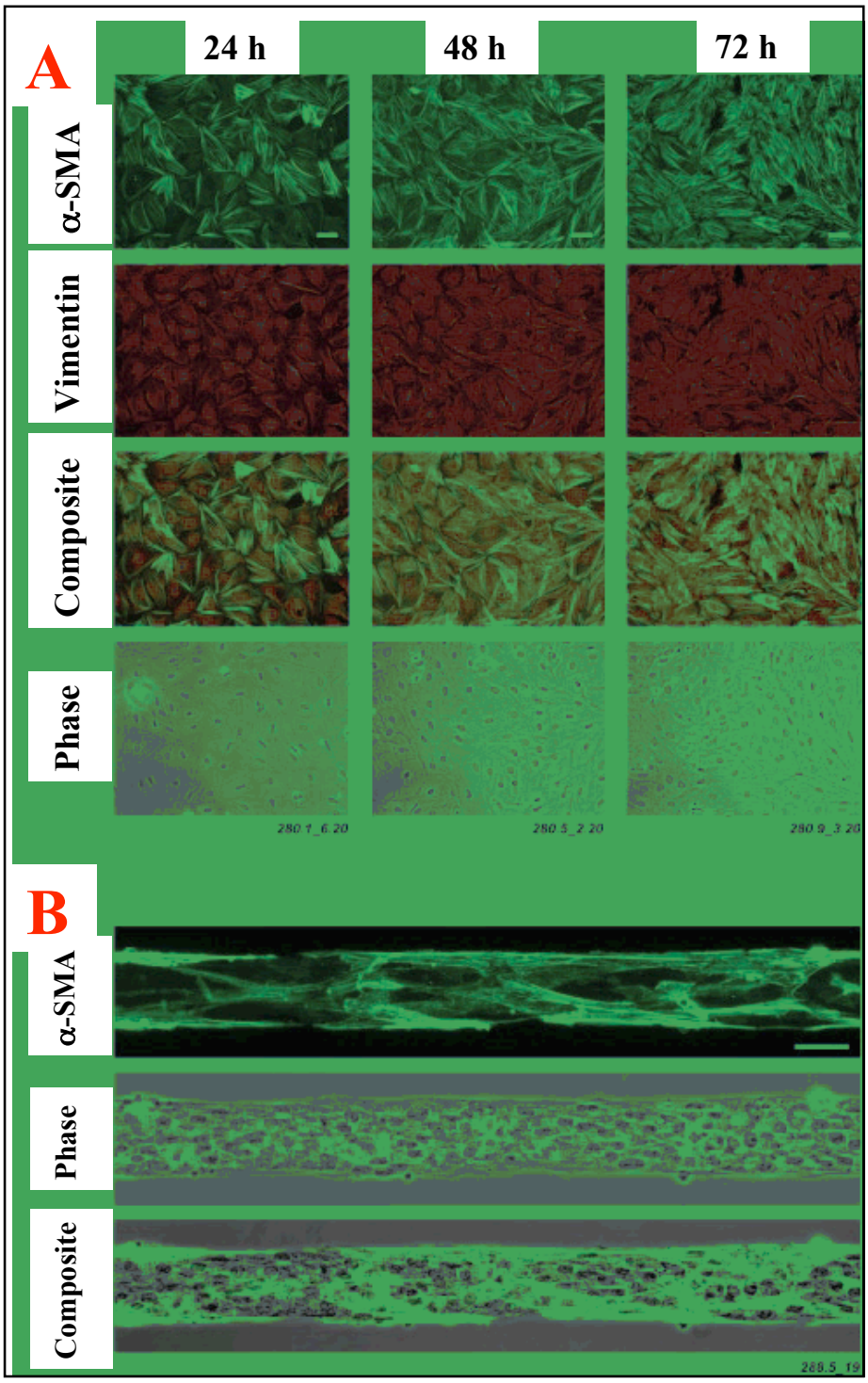


***Figure 5. Phenotype of cultured fibroblasts of cardiac origin.*** *A, Immunofluorescence and phase contrast (phase) images of fibroblast monolayers grown for 24 to 72 hours on glass coverslips. Cells are stained for αSMA and vimentin. Combined expression of both proteins is depicted in the composite images and identifies the cultured fibroblasts as myofibroblasts. Bar =50 µm. B, Similar to cells grown on glass coverslips, fibroblasts cultured on top of cardiomyocyte strands express abundant SMA, which exhibits a stress fiber–like organization. Bar =50 µm.*

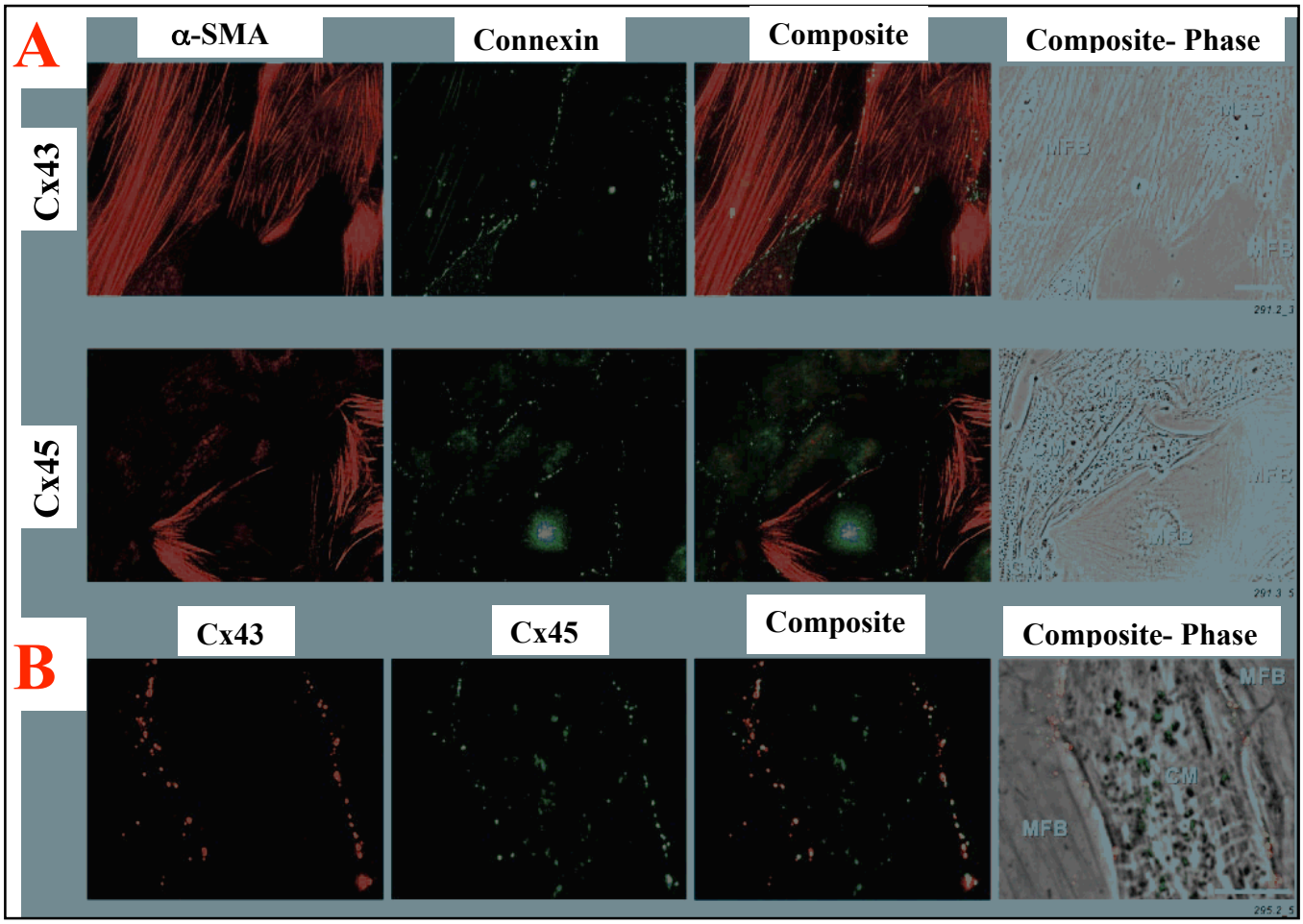


***Figure 6. Homocellular and heterocellular expression of connexins by myofibroblasts.*** *A, Cocultures of cardiomyocytes and fibroblasts were double labeled for αSMA and Cx43 (top row) and Cx45 (bottom row). The composite images show that αSMA-positive cells (myofibroblasts [MFB]) express Cx43 and Cx45 both among themselves and at contact sites with cardiomyocytes (CM). Bar =20 μm. B, Double immunolabeling for Cx43 and Cx45 shows punctate expression of both connexins at heterocellular contact sites. Bar =5 μm.*

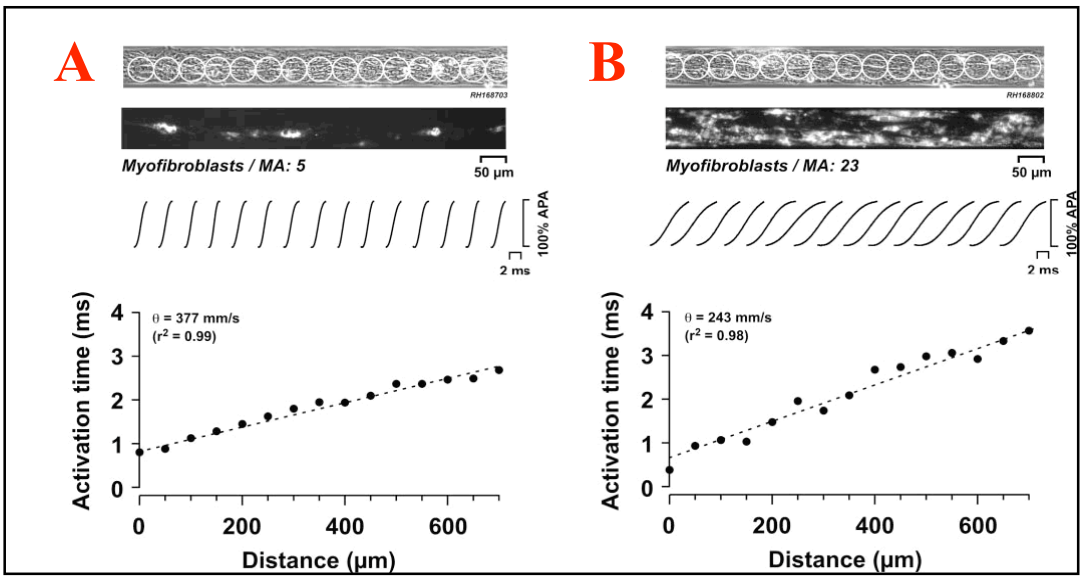


***Figure 7. Impulse conduction characteristics along strands of cardiomyocytes coated with DiI-stained myofibroblasts.*** *A, Top, Phase contrast picture of an 80-µm-wide cardiomyocyte strand with overlaid white circles indicating the positions of individual recording sites. Second panel, Fluorescence image of the same preparation depicting the location of live-stained myofibroblasts within the MA. Third panel, Optically recorded action potential upstrokes along the preparation after stimulation at 2 Hz from the left. Fourth panel, Activation times along the preparation indicate the presence of uniform conduction with a conduction velocity Ø of 377 mm/s (linear least square fit). B, Same as A for a preparation coated by a larger number of myofibroblasts. Maximal upstroke velocities are slowed and Ø is decreased to 243 mm/s.*

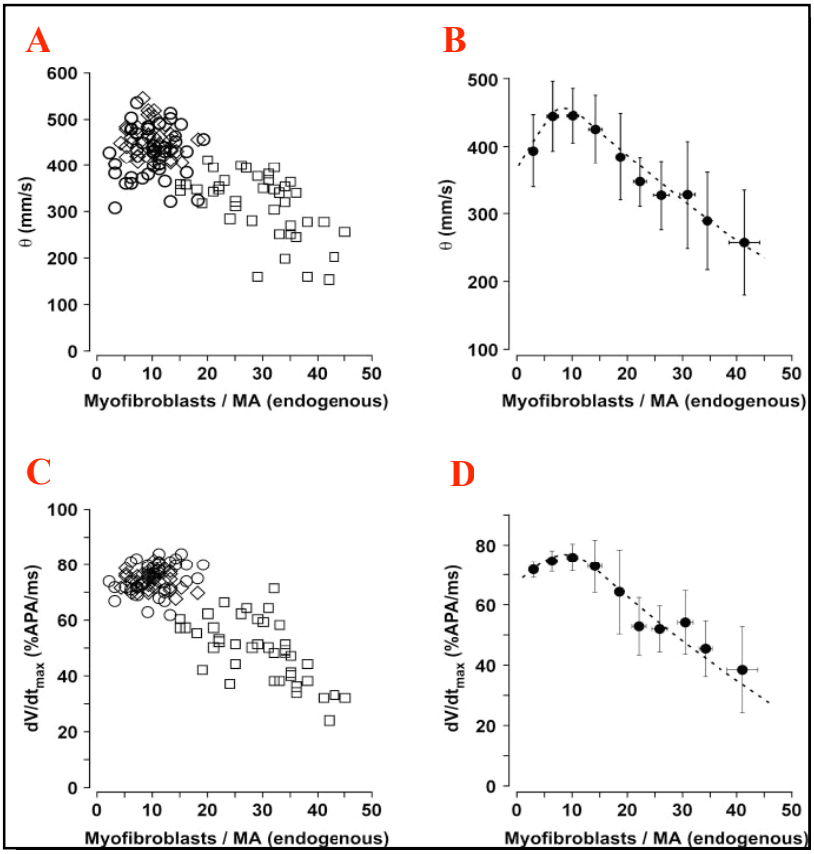


***Figure 8. Dependence of impulse conduction characteristics on the density of the endogenous myofibroblasts.*** *A, Increasing myofibroblast densities cause an initial increase and then a decrease of Ø. Symbols refer to different culture conditions (diamonds indicate preplating + BrdU; circles, preplating only; squares, no preplating, no BrdU). B, Binning of the data of A (bin width= 4) reveals a peak of the biphasic relationship at ≈ 9 myofibroblasts per MA (curve fitted by eye). C and D, Same as A and B for the dependence of $dV/dt_{max}$ of propagated action potentials on myofibroblast density.*

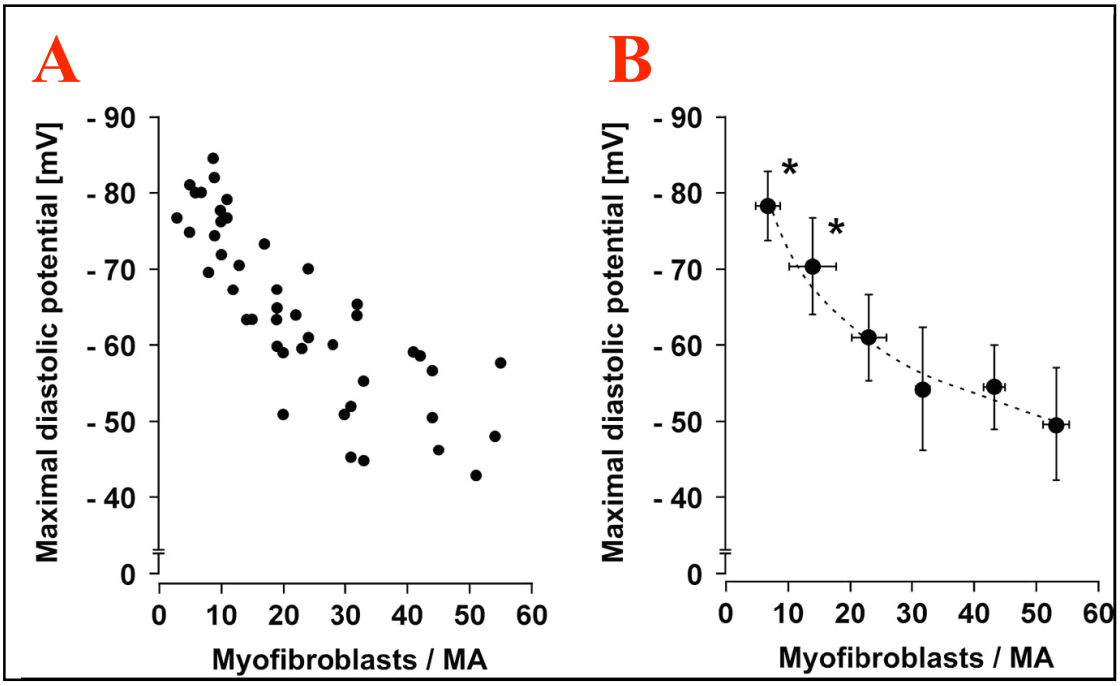


***Figure 9. Dependence of MDPs of cardiomyocyte strands on the density of myofibroblasts.*** *A, Scatter plot of all data. B, Binning of the data in respect to myofibroblast densities (bin width= 10) results in a correlation that is fitted by a power function ($r^2$ = 0.970). Asterisks denote significant differences between consecutive values.*

# Materials and methods

## Primary cell cultures of cardiomyocytes

Patterned growth cell cultures from neonatal rat hearts were prepared according to previously published techniques (Rohr et al., 1998 and 2003). Procedures used were approved by the State Veterinary Department. Hearts from 8 to 10 neonatal rats (Wistar, 1-2 days old) were excised, the ventricles were minced and the resulting small tissue pieces were dissociated in Hank's balanced salt solution (HBSS without $Ca^{2+}$ and $Mg^{2+}$, Bioconcept) containing trypsin (0.1%, Roche Diagnostics) and pancreatin (120 µg/ml, Sigma). The dispersed cells were centrifuged and then resuspended in medium M199 with Hanks' salts (Sigma) containing 10% neonatal calf serum (Bioconcept), streptomycin (20 U/L; Biochrom AG) and vitamin B12 (1,5 µmol/L; Sigma). The cell suspension was preplated for 2 - 2.5 hours under vibration-free conditions in cell culture flasks at a density <1x103 cells/$mm^2$ in order to reduce the percentage of non-myocardial cells. Cardiomyocytes were seeded at a density of 1.6x103 cells/$mm^2$ on coverslips patterned such as to result in 24 monolayer cell strands measuring 0.6 mm x 4.5 mm each. For patch clamp experiments, cardiomyocytes were seeded at ~70 cells/$mm^2$ on collagen coated coverslips (Figure 3). The preparations were grown in supplemented medium M199 containing in addition vitamin C (18 µmol/L; Sigma) and epinephrine (10 µmol/L; Sigma). After 1 day, the medium was exchanged and the serum content was reduced to 5%. Thereafter, medium exchanges were performed every other day.

## Hybrid cell preparations

It was shown before (see introduction) that cultured fibroblasts of cardiac origin undergo a phenotype switch to myofibroblasts within 24 hrs as indicated by the robust expression of α-smooth muscle actin and vimentin (Miragoli et al., 2006). Accordingly, it is denoted cultured fibroblasts as myofibroblasts throughout this study. For obtaining hybrid cell preparations, preplating flasks containing mostly cardiac myofibroblasts (contamination by cardiomyocytes as judged routinely by phase contrast microscopy was < 1%) were kept in culture with supplemented M199

for 8 days before being harvested with trypsin containing dissociation buffer. The resulting cell suspension was centrifuged and resuspended in supplemented medium M199. Myofibroblasts were then seeded at 25 to 950 cells/mm$^2$ onto 1 day old patterned cardiomyocyte preparations. Non-attached cells washed away after 2 hours using supplemented medium M199. In an additional series of experiments, cardiomyocyte strands were coated using identical procedures with wildtype HeLa cells or HeLa cells transfected for connexin 43. Seeding densities were 170 - 340 cells/mm$^2$ for HeLa wildtype cells and 170 - 480 cells/mm$^2$ for Cx43 transfected HeLa cells. After coating with myofibroblasts or HeLa cells, hybrid cell preparations were kept in culture for another 2 - 3 days before undergoing optical determinations of electrical activation patterns.

## Conditioned medium experiments

The effects of medium conditioned by myofibroblasts on spontaneous activity of cardiomyocytes was investigated by closely reproducing the experimental conditions of hybrid cell preparations. For this purpose, 1day old patterned strands of cardiomyocytes were co-incubated with patterned strands (same dimensions) of myofibroblasts for 2-3 days. The two types of preparations were separated by ~ 2 mm from each other in the culture wells by spacers made of platinum wire. In order to permit a sufficient gas exchange in the compartment between the two glass coverslips, the multiwell dishes containing the preparations were gently rotated by a gyratory shaker placed in the incubator during the entire conditioning period (Bio Shaker 3D; lab-4-you).

## Optical recording of electrical activity

After 3 to 4 days in culture, the spatio-temporal characteristics of spontaneous electrical activity was assessed optically after staining the preparations for 5 minutes with the voltage sensitive dye di-8-ANEPPS (135 µmol/L; Biotium). During the experiments, preparations were superfused at 36°C with Hanks' balanced salt solution (HBSS, Sigma) containing (mmol/L) NaCl 137, KCl 5.4, CaCl2 1.3, MgSO4 0.8, NaHCO3 4.2, KH2PO4 0.5, NaH2PO4 0.3 and HEPES 10. The solution was titrated to pH 7.40 with 1 mol/L NaOH and contained 1% serum. In one series of experiments, the surface sarcolemmal KATP-channel opener P-1075 (Tocris) was

added to the superfusion medium at 10 µmol/L in order to force the cells to the equilibrium potential of potassium (Sato et al., 2000). At this concentration, P-1075 has been reported to affect neither rectifying $K^+$ currents nor the L-type $Ca^{2+}$ inward current (Xu et al., 1993). Changes in fluorescence corresponding to transmembrane voltage changes were recorded using a fast CMOS camera (MiCAM Ultima, SciMedia) coupled to a custom made tandem-lens macroscope. This system permitted to record electrical activity in an area measuring 10 mm x 10 mm with a spatial resolution of 100 µm and a temporal resolution of 1 ms. The assessment of spontaneous activity in a given preparation was limited to two recordings lasting 4sec each in order to avoid phototoxic effects of the dyes. Optical raw data were analyzed using dedicated software from the camera manufacturer (BV_Analyze V7.03, SciMedia). After offset correction and digital low-pass filtering of the raw data, the frequency of spontaneous activations and the spatial activation patterns were determined separately for each cardiomyocyte strand and recording with 'n' referring to the total number of these determinations. Cardiomyocyte strands were included in the analysis if they fulfilled the following criteria: (1) the strands had to adhere faithfully to the predefined pattern, (2) the strands had to consist of completely confluent and uniform cardiomyocyte monolayers, and (3), the distribution of coating cells (myofibroblasts and HeLa cells) as assessed by immunocytochemistry following the optical experiments had to be uniform. During the Patch-clamp experiments, the cultured-cells preparations were mounted in a custom-made experimental chamber (Rohr, 1986) and superfused at room temperature with pH-buffered Hanks' balanced salt solution (HBSS, Sigma) containing (mmol/L) NaCl 140, KCl 4, Glucose 5, $CaCl_2$ 2, $MgCl_2$ 1, $NaH_2PO_4$ 2 and HEPES 5 (pH adjusted to 7.4 with NaOH) at 2-3 ml/min.

## Immunocytochemistry and determination of myofibroblast and HeLa cell densities

Following the experiments, preparations were washed with phosphate buffered saline (PBS, Invitrogen) followed by fixation with methanol at -20 ºC for 5 minutes. Thereafter, they were incubated for 20 minutes at room temperature (RT) with blocking buffer (PBS containing 20% goat serum) before being exposed for 2 hours to anti-vimentin (mouse monoclonal, Sigma) dissolved in PBS containing 1% goat

serum and 0.15% triton X-100. After washing, preparations were incubated for 20 minutes at RT with the secondary antibody (Alexa Fluor 488, goat antimouse, Molecular Probes) followed by washing and mounting. The preparations were imaged on an inverted microscope equipped for epifluorescence (Zeiss, Axiovert 200) using a slow-scan camera (Spot RT, Diagnostic Instruments). The spatial extent of coverage of the cardiomyocyte strands with myofibroblasts and HeLa cells was determined using dedicated routines of an image analysis program (ImagePro V 4.5, Media Cybernetics). For this purpose, the locations in the preparations where spontaneous activity started were selected as regions of interest measuring 600 x 600 µm. Within these regions, the percentage area covered by myofibroblasts or HeLa cells was determined after thresholding the data in respect to vimentin fluorescence. On average, these determinations yielded myofibroblast densities of 30.9 ± 13.1 % in myofibroblast coated preparations and 10.7 ± 2.9 % in control preparations (= endogenous myofibroblasts) (Miragoli et al., 2006).

## Whole cell current clamp

The whole cell recording configuration of the patch clamp technique (Figure 5) was used for electrical recordings from single cardiomyocytes using ruptured patches. Patch pipettes were pulled (DMZ-Universal Puller) from borosilicate glass (GC150F-10, Harvard Apparatus). The pipette filling solution contained (mmol/L) K-aspartate 120, NaCl 10, MgATP 3.0, $CaCl_2$ 1.0, EGTA 10; Hepes 5.0; pH = 7.2 (KOH). Pipette resistances ranged from 4 to 6 MOhm. A HEKA patch clamp amplifier (EPC10) was used for current clamp recordings. Analog signals were digitized at 5 KHz and stored on a computer for offline analysis using PatchMaster software (HEKA, version 2.15). Before cell contact, pipette potentials were zeroed. Voltage traces were corrected offline for liquid junction potentials. For the experiments, the cultured cells were mounted in a custom-made experimental chamber (Rohr, 1986) and superfused at RT with pH-buffered Hanks' balanced salt solution at 2-3 ml/min. The resting potentials of the cardiomyocytes used in the analysis were -78.2 ± 6.2 mV with action potential amplitudes averaging 105.2 ± 7.3 (n=15). Input resistances ranged from 1.1 to 2.0 GOhm (average: 1.7 ± 0.3 GOhm). Under current clamp conditions, constant depolarizing current was applied to the cardiomyocytes. The effects of changes in membrane polarization on the likelihood of occurrence of

spontaneous activity was investigated in current clamp mode by injecting 30 sec long constant current pulses of appropriate magnitude and polarization. Using this protocol, was first determined the threshold for occurrence of spontaneous activations and then, during further depolarization of the cells, was recorded the frequency of spontaneous activity as a function of the maximal diastolic potential (Figure 1). Even though constant current injection does not account for dynamic changes in current flow between myofibroblasts and cardiomyocytes during action potentials, it permits to simulate myofibroblast induced changes in diastolic potentials because differences in membrane potentials and, hence, current flow between the two cell types during diastole can be expected to be close to constant. Values are given as mean ± S.D.

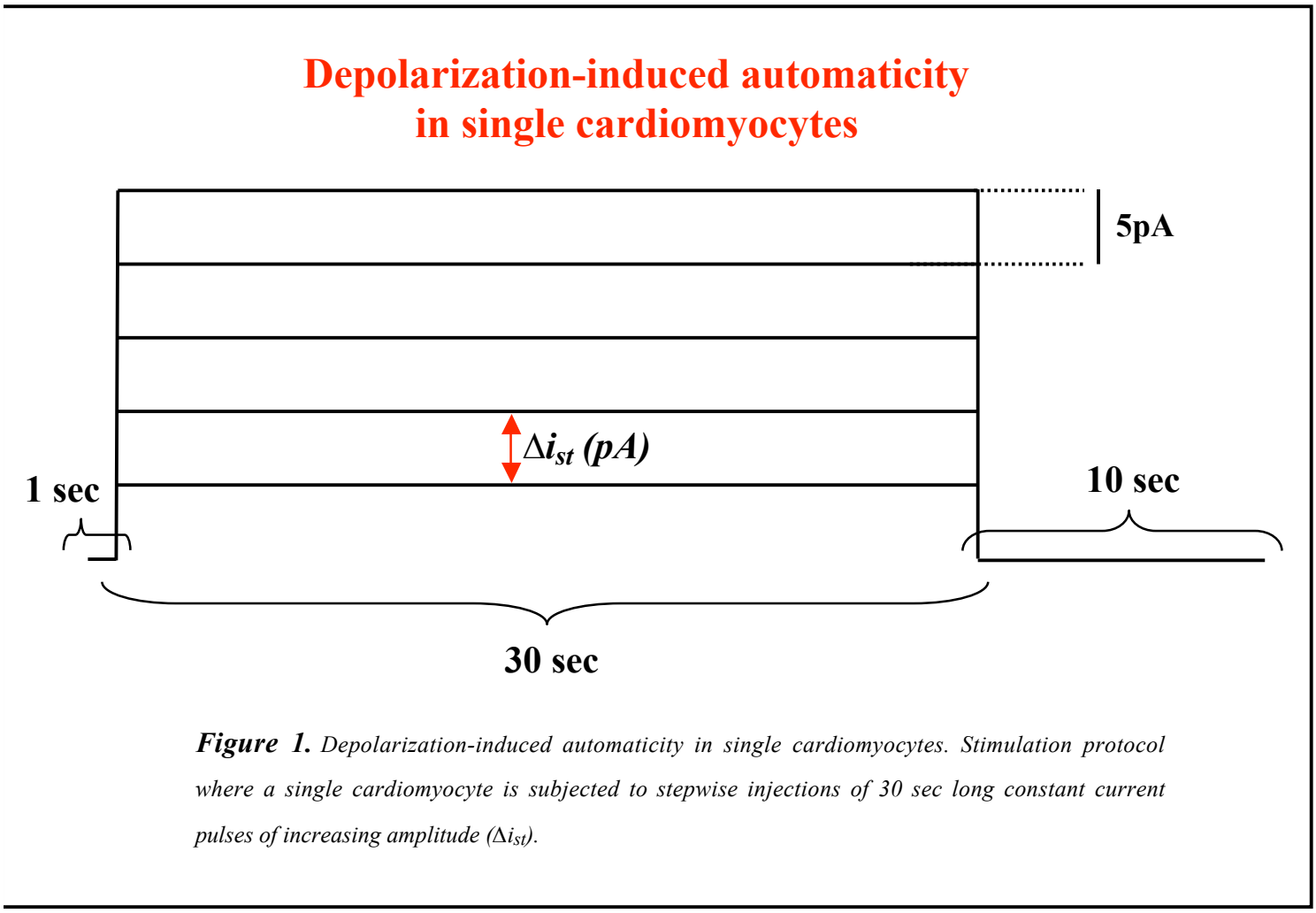


***Figure 1.*** *Depolarization-induced automaticity in single cardiomyocytes. Stimulation protocol where a single cardiomyocyte is subjected to stepwise injections of 30 sec long constant current pulses of increasing amplitude ($\Delta i_{st}$).*

## Myofibroblast density vs. maximal diastolic potentials

It was previously shown using intracellular microelectrode recordings that maximal diastolic potentials in 3-4 day old strands of cardiomyocytes are inversely related to the number of myofibroblasts (Spach et al., 1997). In order to obtain estimates of maximal diastolic potentials as a function of myofibroblast density instead of myofibroblast numbers, these data were reanalyzed by applying image analysis routines as described above to the images of the vimentin stained preparations and correlated these findings to the respective values of maximal diastolic potentials. As shown in figure 1, maximal diastolic potentials of cardiomyocytes were strongly dependent on myofibroblast densities. The power function used to fit the data ($R^2$=0.96) was used to obtain estimates of maximal diastolic potentials in the preparations of this study as presented in Figure 4B and C of this chapter.

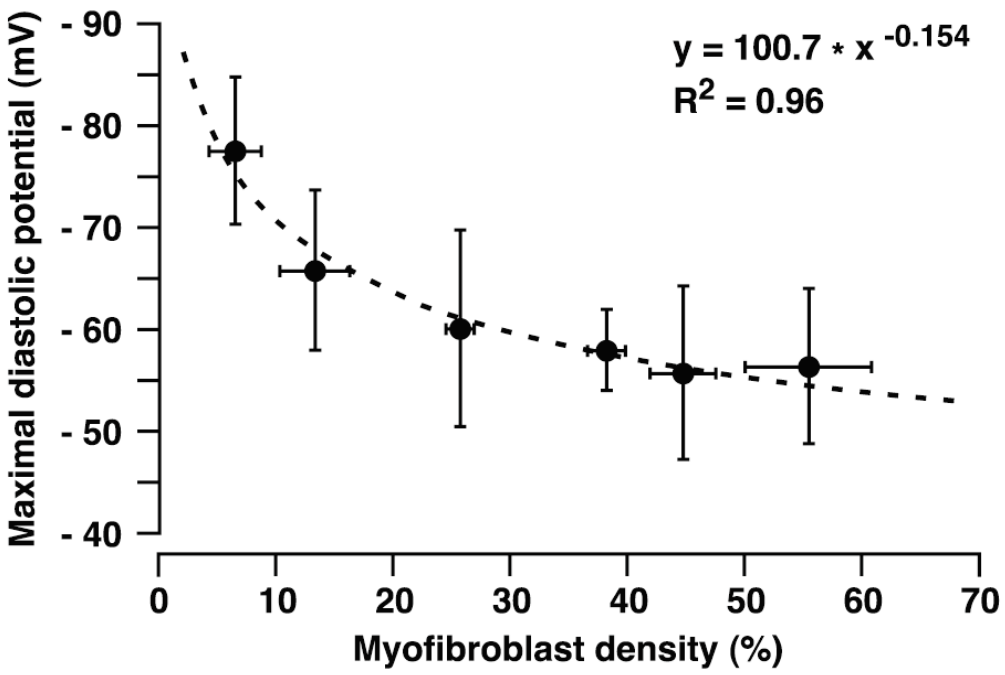


***Figure 2.*** *Dependence of maximal diastolic potentials on myofibroblast density. Values are binned in respect to myofibroblast densities (bin width=10%) and correlated to maximal diastolic potentials of cardiomyocytes recorded with intracellular electrodes in myofibroblast coated cardiomyocyte strands (n=48). The relationship between both parameters is fitted with a power function*

a)

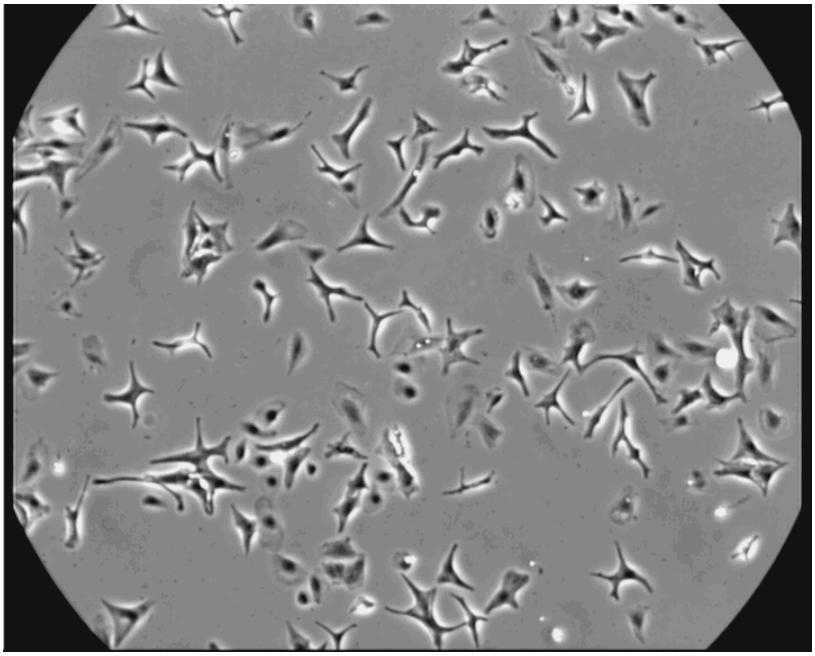

b)

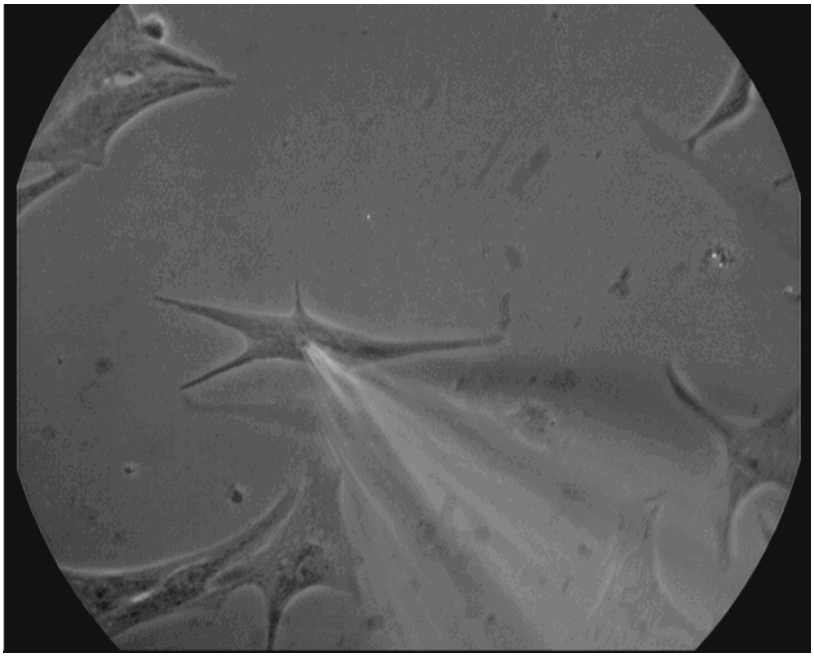

***Fig 3. Neonatal rat ventricular cardyomyocytes seeded on collagen coated coverslips.*** *a) Cardyomyocytes in culture (10x magnification). b) Cardyomyocytes in detail during patch clamp recording (40x magnification).*

a)

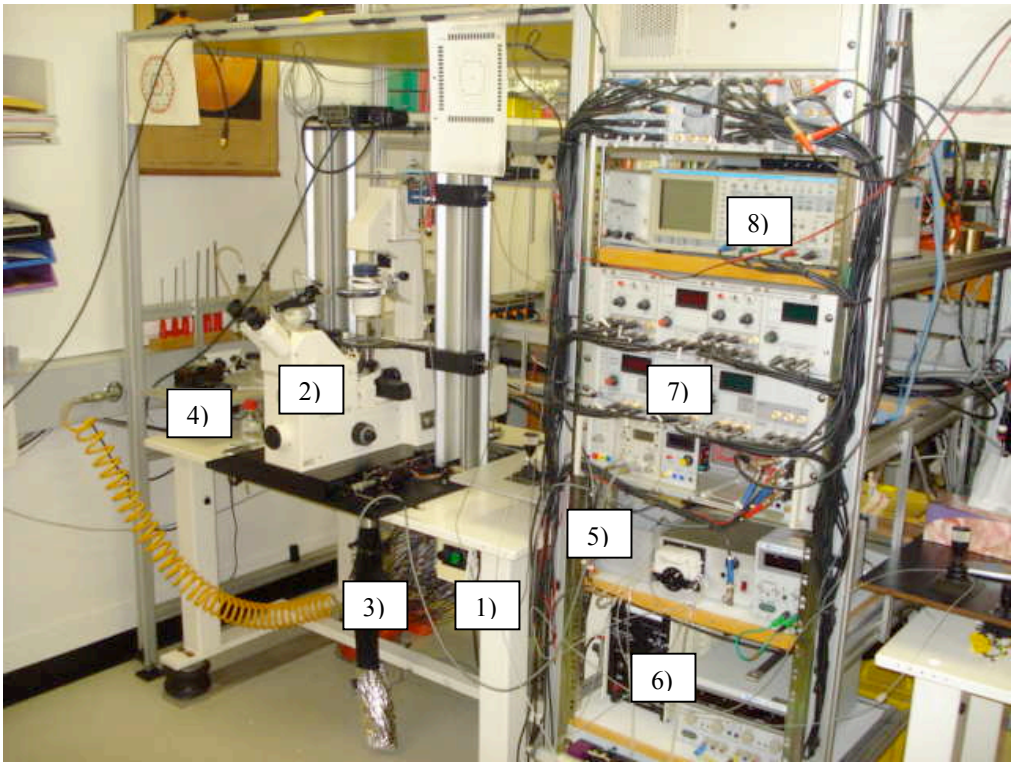


b)

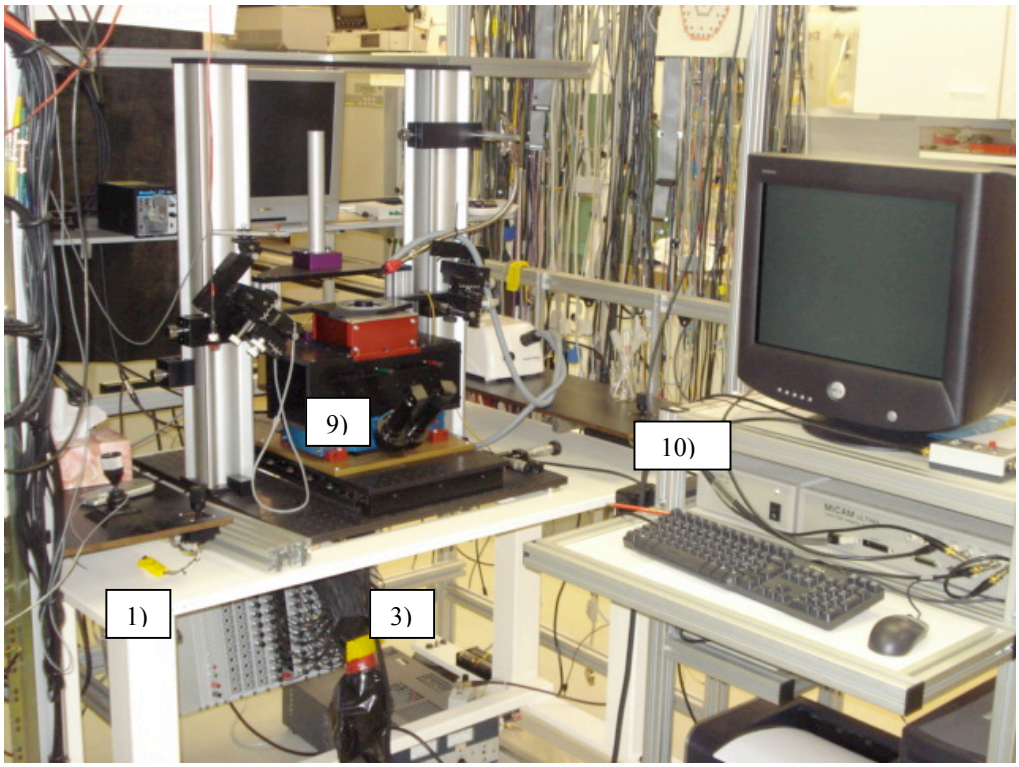


***Fig 4. a) Microscopic and b) macroscopic optical recording setup.*** *Setups are equipped with the following instruments: 1) vibration isolation "xy" table; 2) inverted microscope for epifluorescence adopted for microscopic optical recording; 3) optic fibers; 4) mechanical manipulator; 5) peristaltic pump for temperature control superfusion; 6) power-supply for Xenon Arc Lamp; 7) amplifier and integrator; 8) oscilloscope; 9) macroscopic impulse propagation setup and 10) computer dedicated.*

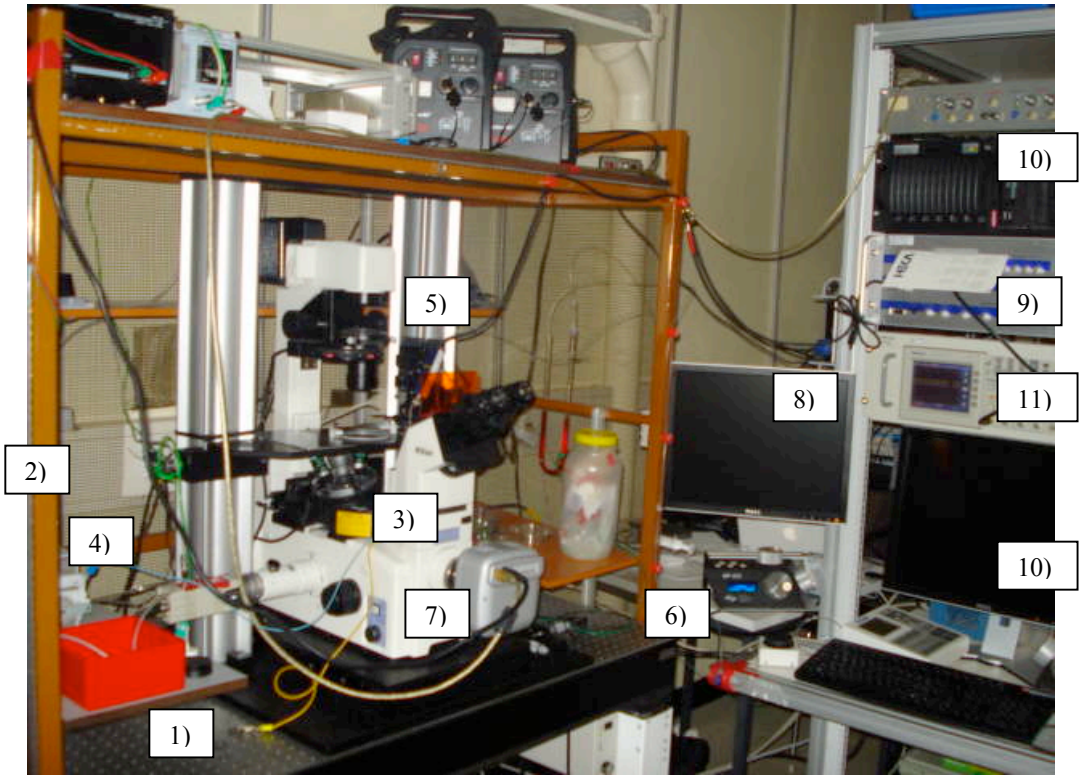


***Fig 5. Patch-clamp setup in the cellular electrophysiology laboratory.*** *Setup is equipped with the following instruments: 1) vibration isolation table; 2) Faraday cage; 3) inverted microscope; 4) pomp for bath perfusion; 5) motorized micromanipulator for recording pipette and 6) controller units for manipulator; 7) video camera and 8) video monitor; 9) patch-clamp amplifier (HEKA EPC 10) and 10) computer dedicated; 11) oscilloscope.*

# Results and discussion

The hypothesis that myofibroblasts might generate abnormal automaticity in cardiac tissue was investigated in patterned growth strands of neonatal rat ventricular cardiomyocytes (Figure 1). Whereas control preparations were invariably quiescent (n=102; Figure 1A,C), coating of the strands with increasing numbers of myofibroblasts (25 to 950 cells/mm$^2$) elicited spontaneous electrical activity in 54.2% of the preparations with an average frequency of 64.4±21.7 min$^{-1}$ (n=548; Figure 1B,C). In contrast, control cardiomyocyte strands cocultured with myofibroblast in a noncontact configuration remained quiescent indicating that induction of spontaneous activity was not dependent on conditioning of the medium by paracrine activity of myofibroblasts (n=333; Figure 1C) (Powell et al., 1999). Spontaneous activations started preferentially at the lateral ends of the strands (83%; Figure 1D) which can be explained by favorable source-to-load conditions offered by these sites. The likelihood of occurrence of synchronized spontaneous activity showed a strong dependence on the density of myofibroblasts (Figure 1E). Whereas preparations were quiescent at myofibroblast densities <15.7%, the percentage of active preparations above this threshold rose to more than 80% at myofibroblast densities of 50%. In parallel, and similar to a recent observation of a decline of activation frequencies in single isolated cardiomyocytes coupled to fibroblasts (Kizana et al., 2006), the frequency of spontaneous activations declined from ≈80 min$^{-1}$ to ≈45 min$^{-1}$ with increasing myofibroblast density. Mechanistically, previous findings showing that myofibroblasts depolarize cardiomyocytes in a cell density dependent manner suggested that myofibroblast induce ectopic activity by ways of depolarization-induced automaticity (Miragoli et al., 2006 and Katzung et al., 1975). Accordingly, we investigated in isolated cardiomyocytes whether the range of membrane depolarizations observed in myofibroblast coated cardiomyocytes is sufficient by itself to induce spontaneous activity. As shown by the patch clamp experiments in Figure 2A, single cultured cardiomyocytes undergoing stepwise depolarizations during injection of 30 s long current pulses of increasing amplitude exhibited depolarization-induced automaticity appearing at membrane potentials less negative than -65 mV. With further depolarization, the frequency of spontaneous activations transiently increased to reach a peak at -56 mV. In a total of 15

cardiomyocytes (Figure 2B; red symbols), spontaneous activity appeared at maximal diastolic potentials (MDPs) less negative than -67.4 mV with >90% of the cells being active at ≈ -55 mV. This voltage dependence is highly similar to that estimated for myofibroblast coated cardiomyocyte strands (Figure 2B; black symbols) which suggests that myofibroblast induced depolarization of cardiomyocyte strands is a major mechanism underlying abnormal automaticity. In further support of this hypothesis, increasing the degree of membrane polarization of myofibroblast coated cardiomyocyte strands by superfusion with the surface sarcolemmal KATP channel opener P-1075 (10 µmol/L, n=43) invariably stopped spontaneous activity. In contrast to the similarities regarding appearance of spontaneous activity as a function of MDP, current-clamped cardiomyocytes showed a biphasic dependence of the frequency of spontaneous activations on MDP (Figure 2C; red symbols) whereas myofibroblast coated cardiomyocyte strands showed a linear decay (Figure 2C; black symbols). This difference likely reflects the circumstance that, in contrast to the frequency response of a given individual cell stepped through different MDPs during patch clamp experiments, the prevailing frequency of multicellular strand preparations is the result of the selection of the fastest pacemaking region capable of driving the load at a given MDP. If spontaneous activity is the result of a partial depolarization of cardiomyocytes by electrotonically coupled myofibroblasts, it should be possible to evoke the same response by coupling cardiomyocytes to other cell types which have an inherently depolarized membrane potential and establish heterocellular gap junctional coupling with cardiomyocytes. This hypothesis was investigated by coating strands of cardiomyocytes with communication deficient HeLa wildtype cells (HeLawt; resting potentials ≈ -40 mV) (Roy et al., 2006) and HeLa cells transfected with connexin 43 (HeLaCx43) which are able to establish functional heterocellular gap junctional coupling with cardiomyocytes (Gaudesius et al., 2003). As shown in Figure 3, coating of cardiomyocyte strands with HeLawt cells failed to induce automaticity even though cell densities reached nearly 100% (n=203). In contrast, coating of cardiomyocyte strands with HeLaCx43 cells elicited spontaneous electrical activity at cell densities >39.5% with maximal effects (≈ 80% spontaneously active strands) observed at densities of 80%. Average activation rates (58.4±26.2 $min^{-1}$, n=233) showed no significant dependence on HeLaCx43 cell

density (data not shown). As for the case of myofibroblasts, activations started preferentially at the lateral ends of the strands (89%).

## Discussion

Abnormal electrical activity based on depolarization-induced automaticity is a well established arrhythmogenic mechanism thought to occur, eg, in the context of injury currents flowing across the border zones of acute infarcts (Carmeliet et al., 1999). Whereas this type of ectopic activity is dependent on spatial heterogeneities of electrophysiological properties within homocellular networks of cardiomyocytes, the results of the present study demonstrate that depolarization-induced automaticity can similarly be induced by heterocellular electrotonic interactions between cardiomyocytes and communication competent but less polarized cells like myofibroblasts and HeLaCx43 cells. For monolayer cultures of cardiomyocytes, these findings demonstrate that spontaneous activity is not, as commonly assumed, due to a culture-dependent dedifferentiation of cardiomyocyte toward a spontaneously active immature phenotype, but is the specific result of electrotonic interactions with a sufficient number of myofibroblasts. As a consequence, the interpretation of beat rate changes in these preparations following specific experimental interventions need to take into account the possibility that observed effects are not necessarily cardiomyocyte-related but might occur secondary to a modification of the electrophysiology of myofibroblasts. In regard to intact cardiac tissue, the findings of this study open the perspective that contact regions between cardiomyocytes and sufficiently large numbers of myofibroblasts as occurring in the borderzone of healing infarcts (Sun et al., 2002) a few days after the acute event or in the fibrotic working myocardium (Clement et al., 1999) might give rise to arrhythmogenic ectopic activity. Proof of this hypothesis is pending confirmation that myofibroblasts in vivo retain an electrophysiological phenotype similar to that in culture and that their capacity to depolarize adjacent cardiomyocytes is sufficient to induce ectopic activity. Finally, the findings suggest that transplantation of communication competent cells exhibiting a reduced resting membrane potential like undifferentiated human mesenchymal stem cells (Heubach et al., 2004) might bear the potential to induce ectopic activity independent on their ability to produce regenerative activity.

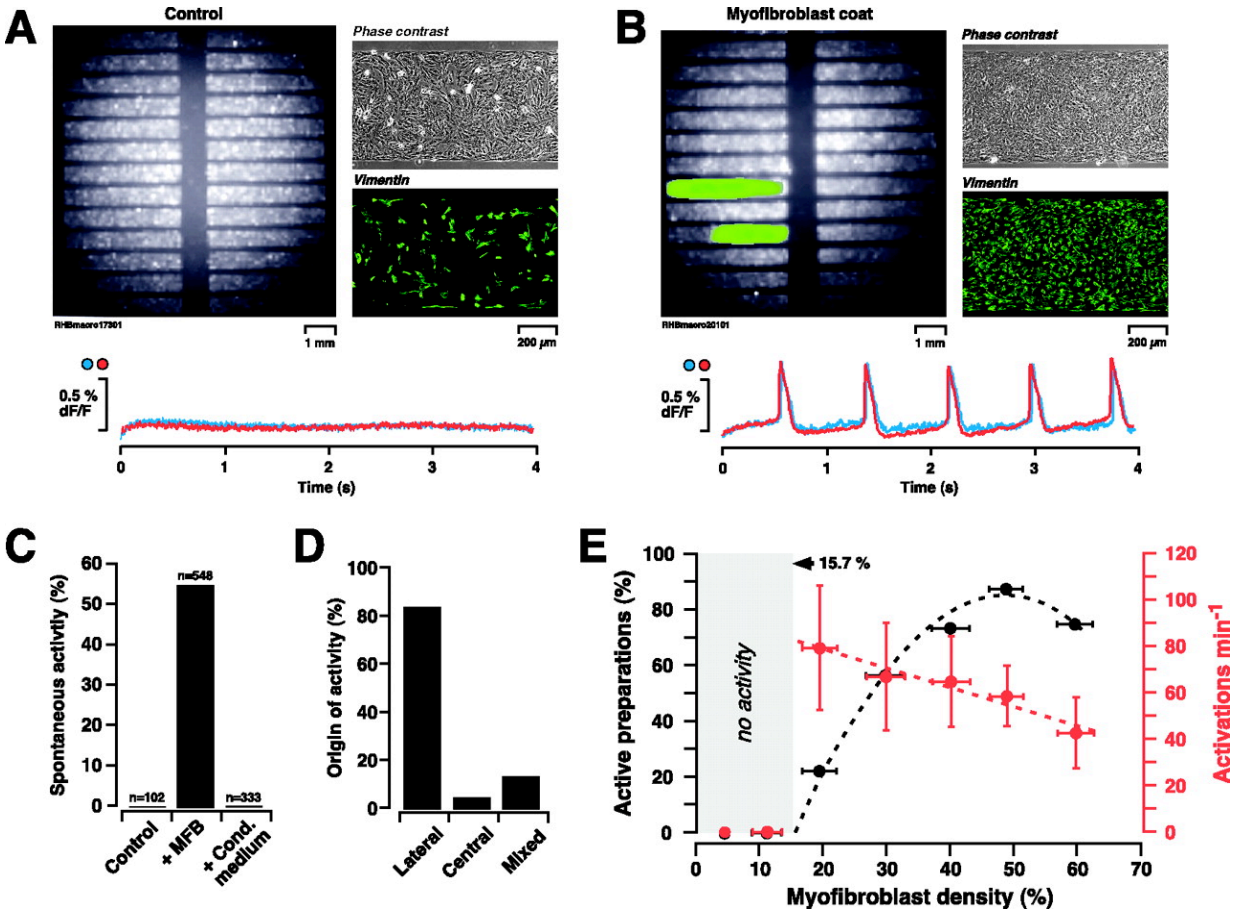


***Figure 1. Induction of spontaneous activity in strands of cardiomyocytes by myofibroblasts.*** *A, Overview of a control preparation consisting of strands of cardiomyocytes measuring 4.5x0.6 mm each. The cellular microarchitecture (phase contrast) and the density and distribution of endogenous myofibroblasts (vimentin staining) of one strand are shown at higher magnification on the right. Below, optical recordings from two locations denoted with a blue and red disc in the overview show absence of spontaneous activity. B, Same as A for a preparation which was coated with myofibroblasts. Propagating activations are shown in green. The strand denoted with colored discs exhibited spontaneous activity at 1.2 Hz. C, Incidence of spontaneous activity in control preparations, preparations coated with myofibroblasts, and preparations incubated with myofibroblast conditioned medium. D, Localization of ectopic foci in myofibroblast coated spontaneously active preparations. E, Percentage of active preparations (left ordinate, black; binomial fit: $R^2$=0.98) and frequency of activity (right ordinate, red; linear fit: $R^2$=0.94) as a function of myofibroblast density. Data are binned (bin width=10%). (Activation movies of the preparations 1A and 1B are available in the online data supplement at http://circres.ahajournals.org.)*

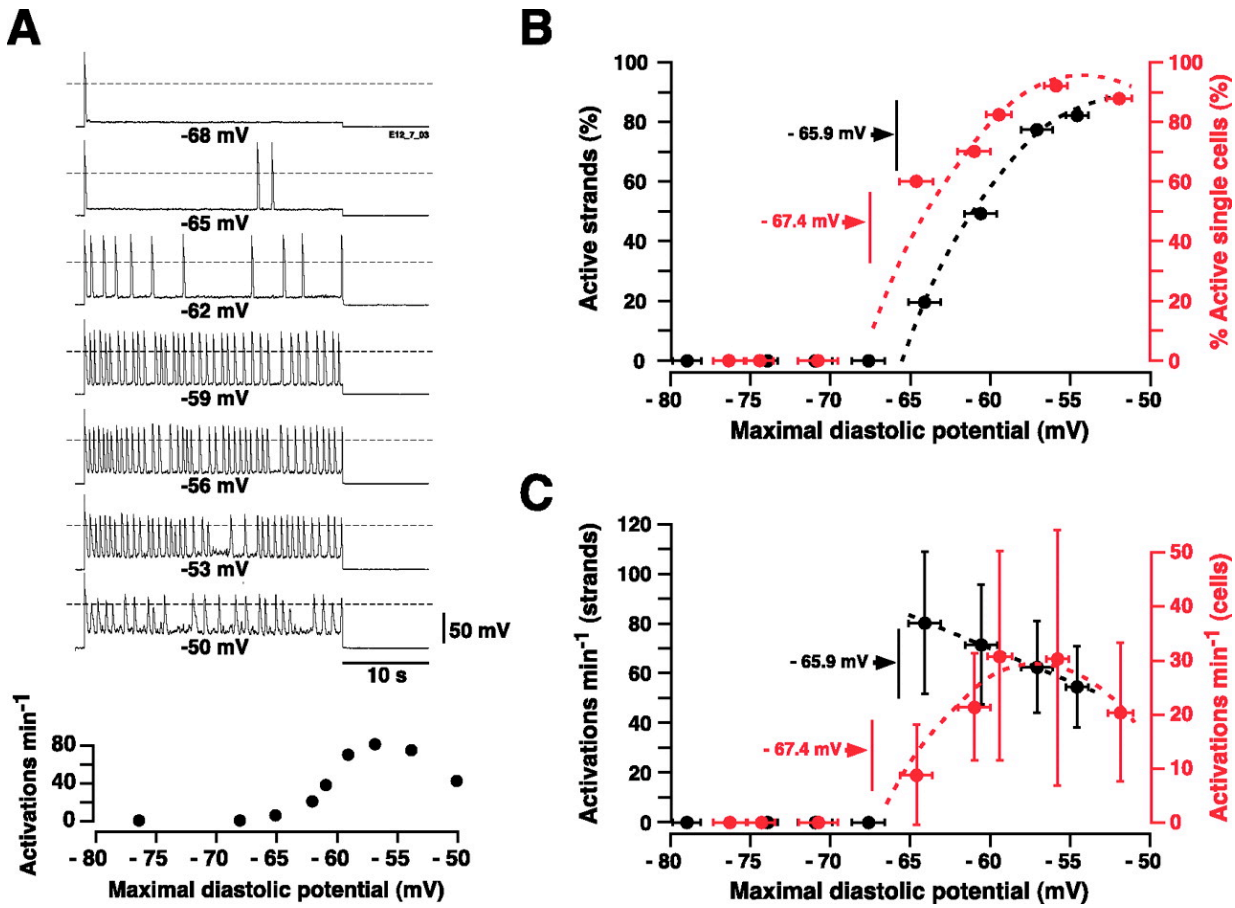


***Figure 2. Depolarization-induced automaticity in single cardiomyocytes.*** *A, Spontaneous activity in a single cardiomyocyte being current-clamped to increasingly depolarized potentials. B, Dependence of the likelihood of occurrence of spontaneous activity on maximal diastolic potentials (MDP) for current clamped single cardiomyocytes (red symbols; n=15; binomial fit: $R^2$=0.94) and myofibroblast coated cardiomyocyte strands (black symbols; n=300; polynomial fit: $R^2$=0.99). Data were binned (bin width=3.5 mV) and values with arrows indicate threshold potentials for occurrence of spontaneous activity for the two types of preparations. C, Same as B for the dependence of frequency of spontaneous activations on MDP (red: binomial fit, $R^2$=0.94; black: linear fit, $R^2$=0.99).*

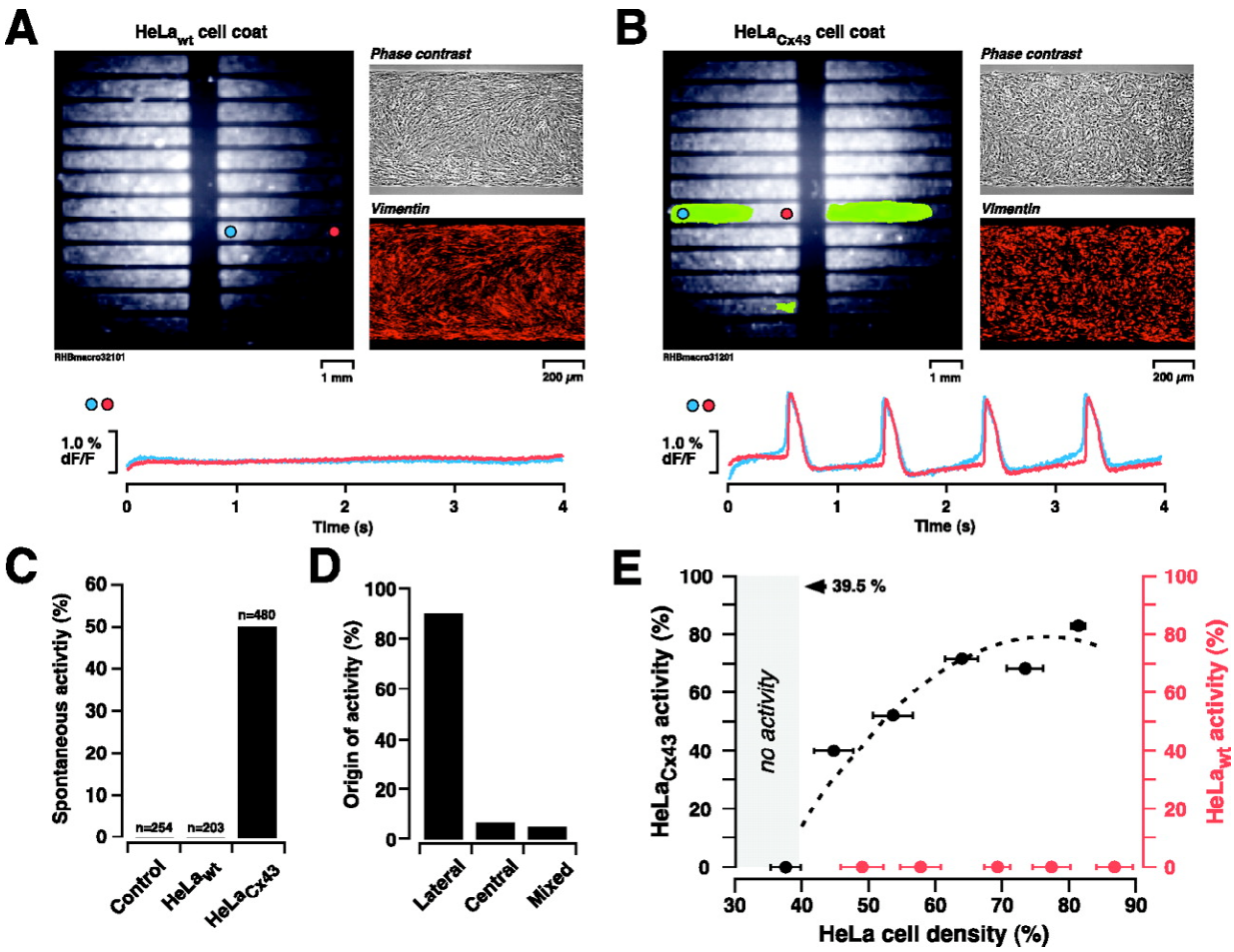


***Figure 3. Induction of spontaneous activity by HeLa cells.*** *A, Overview of a preparation coated with HeLawt cells. The cellular microarchitecture (phase contrast) and the density and distribution of HeLawt cells (vimentin staining) are shown on the right. The optical recording below shows absence of spontaneous activity at the two locations denoted with a blue and red disc in the overview. B, Same as A for a preparation which was coated with HeLaCx43 cells. Propagating activations are shown in green. The strand denoted with colored discs was spontaneously active at 1.1 Hz. C, Incidence of spontaneous activity in control preparations and preparations coated with HeLawt and HeLaCx43 cells, respectively. D, Localization of ectopic foci in spontaneously active preparations. E: Percentage of active preparations with HeLaCx43 coating (left ordinate, black; polynomial curve fit: R2=0.94) and with HeLawt coating (right ordinate, red) as a function of HeLa cell density. (Activation movies of the preparations 3A and 3B are available in the online data supplement at http://circres.ahajournals.org.)*

# References

**Abraham MR, Henrikson CA, Tung L, et al.** Antiarrhythmic engineering of skeletal myoblasts for cardiac transplantation. *Circ Res.* 2005;97(2):159-167.

**Avila G, Medina IM, Jimenez E, et al.** Transforming growth factor-beta1 decreases cardiac muscle L-type Ca2+ current and charge movement by acting on the Cav1.2 mRNA. *Am J Physiol.* 2007;292(1):H622-631.

**Burrows MT.** Rhythmische Kontraktionen der isolierten Hermuskelzelle ausserhalb des Organismus. *Munchener Medizinische Wochenschrift.* 1912;27:1-3.

**Camelliti P, Devlin GP, Matthews KG, et al.** Spatially and temporally distinct expression of fibroblast connexins after sheep ventricular infarction. *Cardiovas Res.* 2004;62(2):415.

**Carmeliet E.** Cardiac ionic currents and acute ischemia: from channels to arrhythmias. *Physiol Rev*. 1999;79:917–1017.

**Clement S, Chaponnier C, Gabbiani G.** A subpopulation of cardiomyocytes expressing α-skeletal actin is identified by a specific polyclonal antibody. *Circ Res.* 1999;85:51e– e58.

**Coronel R, Wilms-Schopman FJ, Opthof T, et al.** Injury current and gradients of diastolic stimulation threshold, TQ potential, and extracellular potassium concentration during acute regional ischemia in the isolated perfused pig heart. *Circ Res.* 1991;68(5):1241-1249.

**Coronel R, Wilms-Schopman FJG, deGroot JR.** Origin of ischemia-induced phase 1b ventricular arrhythmias in pig hearts. *J Am Coll Cardiol.* 2002;39(1):166-176.

**Coutu P, Chartier D, Nattel S.** Comparison of Ca2+-handling properties of canine pulmonary vein and left atrial cardiomyocytes. *Am J Physiol.* 2006;291(5):H2290-

2300.

**Feld Y, Melamed-Frank M, Kehat I, Tal D, Marom S, Gepstein L.** Electrophysiological modulation of cardiomyocytic tissue by transfected fibroblasts expressing potassium channels: a novel strategy to manipulate excitability. *Circulation*. 2002;105:522–529.

**Gaudesius G, Miragoli M, Thomas SP, Rohr S.** Coupling of cardiac electrical activity over extended distances by fibroblasts of cardiac origin. *Circ Res*. 2003;93:421– 428.

**Gabbiani G, Chaponnier C, Huttner I.** Cytoplasmic filaments and gap junctions in epithelial cells and myofibroblasts during wound healing. *J Cell Biol.* 1978;76(3):561-568.

**Gabbiani G.** The myofibroblast in wound healing and fibrocontractive diseases. *J Pathol.* 2003;200:500-503.

**Goldsmith EC, Hoffman A, Morales MO, Potts JD, Price RL, McFadden A, Rice M, Borg TK.** Organization of fibroblasts in the heart. *Dev Dyn*. 2004;230.

**Gorenek B, Kudaiberdieva G, Birdane A, et al.** Initiation of monomorphic ventricular tachycardia: electrophysiological, clinical features, and drug therapy in patients with implantable defibrillators. *J Electrocardiol.* 2003;36:213-218.

**Heubach JF, Graf EM, Leutheuser J, Bock M, Balana B, Zahanich I, Christ T, Boxberger S, Wettwer E, Ravens U.** Electrophysiological properties of human mesenchymal stem cells. *J Physiol*. 2004;554:659–672.

**Hyde A, Blondel B, Matter A, Cheneval JP, Filloux B, Girardier L.** Homo- and heterocellular junctions in cell cultures: an electrophysiological and morphological study. *Prog Brain Res*. 1969;31:283–311.

**Huelsing DJ, Spitzer KW, Pollard AE.** Spontaneous activity induced in rabbit Purkinje myocytes during coupling to a depolarized model cell. *Cardiovas Res.*

2003;59(3):620.

**Katzung BG.** Effects of extracellular calcium and sodium on depolarization-induced automaticity in guinea pig papillary muscle. *Circ Res*. 1975;37:118 –127.

**Kawada H, Niwano S, Niwano H, et al.** Tumor necrosis factor-• downregulates the voltage gated outward K+ current in cultured neonatal rat cardiomyocytes. *Circ J (Jap)*. 2006;70:605-609.

**Kizana E, Ginn SL, Boyd A, Thomas SP, Allen DG, Ross DL, Alexander IE.** Fibroblasts modulate cardiomyocyte excitability: implications for cardiac gene therapy. *Gene Therapy*. 2006;13:1611–1615.

**Kohl P, Kamkin AG, Kiseleva IS, Nobel D.** Mechanosensitive fibroblasts in the sino-atrial node region of rat heart: interactions with cardiomyocytes and possible role. *Exp Physiol*. 1994;79:943–956.

**Lefroy DC, Fang JC, Stevenson LW, Hartley LH, Friedman PL, Stevenson WG.** Recipient-to-donor atrioatrial conduction after orthotopic heart transplantation: surface electrocardiographic features and estimated prevalence. *Am J Cardiol*. 1998;82:444–450.

**Manabe I, T. S, Nagai R.** Gene expression in fibroblasts and fibrosis. *Circ Res.* 2002;91:1103-1113.

**McAnulty RJ, Laurent GJ.** Collagen synthesis and degradation in vivo. Evidence for rapid rates of collagen turnover with extensive degradation of newly synthesized collagen in tissues of the adult rat. *Coll Relat Res.* 1987;7(2):93-104.

**Miragoli M, Gaudesius G, Rohr S.** Electrotonic modulation of cardiac impulse conduction by myofibroblasts. *Circ Res.* 2006;98(6):801-810.

**Peters NS, Wit AL.** Myocardial architecture and ventricular arrhythmogenesis. *Circ.*

1998;97(17):1746-1754.

**Powell DW, Mifflin RC, Valentich JD, Crowe SE, Saada JI, West AB.** Myofibroblasts. I. Paracrine cells important in health and disease. *Am J Physiol*. 1999;277:C1–C19.

**Rohr S.** Temperature-controlled perfusion chamber suited for mounting on microscope stages. *J Physiol (London).* 1986;378:90p.

**Rohr S, and Kucera J.P.** Optical recording system based on a fiber optic image conduit: Assessment of microscopic activation patterns in cardiac tissue. *Biophys J.* 1998;75(2):1062-75.

**Rohr S, Flückiger-Labrada R, Kucera J.P.** Photolithographically defined deposition of attachment factors as a versatile method for patterning the growth of different cell types in culture. *Eur J Physiol.* 2003;446:125-132.

**Rook MB, Jongsma HJ, de Jonge B.** Single channel currents of homo- and heterologous gap junctions between cardiac fibroblasts and myocytes. *Pflugers Arch.* 1989;414:95-98.

**Roy G, Sauvè R.** Stable membrane potentials and mechanical $K^+$ responses activated by internal $Ca^{2+}$ in HeLa cells. *Can J Physiol Pharmacol*. 1983;61:144 –148.

**Rubart M, Zipes DP.** Mechanisms of sudden cardiac death. *J Clin Invest.* 2005;115:2305-2315.

**Sato T, Sasaki N, Seharaseyon J, O'Rourke B, Marban E.** Selective pharmacological agents implicate mitochondrial but not sarcolemmal KATP channels in ischemic cardioprotection. *Circulation.* 2000;101(20):2418-2423.

**Shaw R, Rudy Y.** Electrophysiologic effects of acute myocardial ischemia. A mechanistic investigation of action potential conduction and conduction failure. *Circ*

*Res.* 1997;80:124-138.

**Spach MS, Boineau JP.** Microfibrosis produces electrical load variations due to loss of side-to-side cell connections: A major mechanism of structural heart disease arrhythmias. *Pace*. 1997;20:397– 413.

**Sun Y, Weber KT.** Angiotensin converting enzyme and myofibroblasts during tissue repair in the rat heart. *J Mol Cell Cardiol.* 1996;28:851-858.

**Sun Y, Kiani MF, Postlethwaite AE, Weber KT**. Infarct scar as living tissue. *Basic Res Cardiol*. 2002;97:343–347.

**Sun H, Kerfant B-G, Zhao D, et al.** Insulin-like growth factor-1 and PTEN deletion enhance cardiac L-type Ca2+ currents via increased PI3Ka/PKB signaling. *Circ Res.* 2006;98(11):1390-1397.

**Swynghedauw B.** Molecular mechanisms of myocardial remodeling. *Physiol Rev*. 1999;79:215–262.

**Tokuda K, Kai H, Kuwahara F, et al.** Pressure-independent effects of angiotensin II on hypertensive myocardial fibrosis. *Hypertension.* 2004;43(2):499-503.

**Tomasek JJ, Gabbiani G, Hinz B, et al.** Myofibroblasts and mechanoregulation of connective tissue remodelling. *Nat Rev Mol Cell Biol.* 2002;3(5):349-363.

**Tsai C-F, Tai C-T, Hsieh M-H, et al.** Initiation of atrial fibrillation by ectopic beats originating from the superior vena cava: electrophysiological characteristics and results of radiofrequency ablation. *Circ.* 2000;102(1):67-74.

**Weber KT.** Fibrosis and hypertensive heart disease. *Curr Opin Cardiol.* 2000;15:264-272.

**Weber KT.** Fibrosis in hypertensive heart disease: focus on cardiac fibroblasts. *J*

*Hypertens*. 2004;22:47–50.

**Yano M, Ikeda Y, Matsuzaki M.** Altered intracellular Ca2+ handling in heart failure. *J Clin Invest.* 2005;115(3):556-564.

**Xu X, Tsai TD, Lee KS.** A specific activator of the ATP-inhibited K+ channels in guinea pig ventricular cells. *J Pharmacol. Exp. Ther.* 1993;266(2):978-984.

**Xue T, Cho HC, Akar FG, et al.** Functional integration of electrically active cardiac derivatives from genetically engineered human embryonic stem cells with quiescent recipient ventricular cardiomyocytes: insights into the development of cell-based pacemakers. *Circ.* 2005;111(1):11-20.